

POSTPRINT (PEER-REVIEWED, PUBLISHED, JOURNAL-TYPESET COPY)

This manuscript is a **postprint** uploaded to EarthArXiv. It has been peer-reviewed and published in **BASIN RESEARCH** on the **18/01/2019**, and has the DOI **10.1111/bre.12341**. Authors welcome comments, feedback, and discussions anytime.

Feel free to get in contact: geo.david.fernandez@gmail.com

Monoclinal flexure of an orogenic plateau margin during subduction, south Turkey

David Fernández-Blanco¹  | Giovanni Bertotti¹ | Ali Aksu² | Jeremy Hall²

¹Department of Geotechnology, Faculty of Civil Engineering and Geosciences, Delft University of Technology, Delft, The Netherlands

²Department of Earth Sciences, Centre for Earth Resources Research, Memorial University of Newfoundland, St. John's, Newfoundland, Canada

Correspondence

David Fernández-Blanco, Department of Geotechnology, Faculty of Civil Engineering and Geosciences, Delft University of Technology, Delft, The Netherlands.

Email: geo.david.fernandez@gmail.com

Funding information

855.01.142 (07-TOPO-EUROPE-FP-013), Grant/Award Number: Miocene tectonics in the Central Anatolia Plateau; Netherlands Organisation for Scientific Research; Natural Sciences and Engineering Research Council of Canada

The copyright line for this article was changed on 31 January after original online publication

Abstract

Geologic evidence across orogenic plateau margins enables the discrimination of the relative contributions of orogenic, epeirogenic and/or climatic processes that lead to growth and maintenance of those plateaus and their margins. Here, we discuss the mode of formation of the southern margin of the Central Anatolian Plateau (SCAP) and evaluate its time of formation using fieldwork in the onshore and seismic reflection data in the offshore. In the onshore, uplifted Miocene rocks in a dip-slope topography show monocline flexure over >100 km, km-scale asymmetric folds verging south, and outcrop-scale syn-sedimentary reverse faults. On the Turkish shelf, vertical faults transect the basal latest Messinian of a 10 km fold where on-structure syn-tectonic wedges and synsedimentary unconformities indicate pre-Pliocene uplift and erosion, followed by Pliocene and younger deformation. Collectively, Miocene rocks delineate a flexural monocline at plateau margin scale that is expressed along our on-offshore sections as a kink-band fold with a steep flank 20–25 km long. In these reconstructed sections, we estimate a relative vertical displacement of 3.8 km at rates of ca. 0.5 mm/y, and horizontal shortening values <1 %. We use this evidence together with our observations of shortening at outcrop, basin, plateau-margin and forearc-system scales to infer that the SCAP forms as a monoclinial flexure to accommodate deep-seated thickening and shortening since >5 Ma, and to contextualize the plateau margin as the forearc high of the Cyprus subduction system.

KEYWORDS

Anatolian plateau, Cilicia Basin, monocline, Mut Basin, orogenic plateau, plateau margin, south Turkey

1 | INTRODUCTION

Many mechanisms are proposed to explain the growth of orogenic plateaus and the long-term feedbacks between their geodynamic and/or climatic controls (e.g. Bird, 1979; Powell, 1986; Nelson et al., 1996; Pope & Willett, 1998; Yin & Harrison, 2000; Tapponnier et al., 2001; Şengör, Özeren, Genç, & Zor, 2003; Sobel, Hilley, & Strecker, 2003; Rowley & Currie, 2006; Garcia-Castellanos, 2007;

Ballato et al., 2010; Biryol, Beck, Zandt, & Özacar, 2011). While tectono-structural and thermo-mechanical models relate plateau margin growth to accretion/removal of crustal or lithospheric material, magmatic/tectonic underplating or rheological changes (e.g. Allmendinger, Jordan, Kay, & Isacks, 1997; Clark, 2012), the climatic-erodibility models relate the tectonic activity to climate, rock erodibility and precipitation power during incipient relief development (e.g. Mulch, Graham, & Chamberlain, 2006; Strecker et al., 2009).

Geologic data across plateau margins (on- and offshore) is pivotal to understand plateau margin growth and explain certain features that are not always entirely captured by these models.

Current studies advocate for epeirogenic causes to explain the growth and uplift of the Central Anatolian Plateau southern margin (SCAP) (e.g. Schildgen, Yıldırım, Cosentino, & Strecker, 2014). Shallow slab break-off and asthenospheric mantle upwelling are proposed as engines for the post-8 Ma surface uplift of the modern Central Taurides, occurring either separately from (Cosentino et al., 2012), or jointly with, a second uplift phase, with rates of 0.6–0.7 mm/year and leading to 1,200 m of topography after 1.6 Ma (Schildgen et al., 2012), and a new uplift phase, with rates of 3.21–3.42 mm/year and leading to up to 1,500 m of topography, since 450 ka (Öğretmen et al., 2018). For these studies, the Central Taurides surface uplift is ‘passive’ and detached from regional compression due to subduction (e.g. Schildgen et al., 2014).

Epeirogenic models of plateau uplift that might apply in the Central Anatolia Plateau interior (e.g. Bartol & Govers, 2014; Göğüş, Pysklywec, Şengör, & Gün, 2017) are at variance with geologic evidence farther south. For example, the Cyprus slab is imaged by tomography along the Central Cyprus subduction zone and below the modern Central

Highlights

- Onshore and offshore data contextualise south Turkey as the forearc high of the Central Cyprus forearc system.
- The Central Anatolian Plateau southern margin (SCAP) results from compressional growth of a Miocene monocline.
- SCAP monocline is a kink-band with a steep flank (20 km horizontally; 3.8 km vertically) and <1% shortening.
- SCAP vertical tectonic motions started >5 Ma, and relevant relief existed in the modern Central Taurides ca. 5 Ma.
- We propose plateau margin growth by subduction margin accretion in the Central Cyprus forearc and crustal thickening.

Taurides (e.g. Bakırcı, Yoshizawa, & Özer, 2012; Abgarmi et al., 2017), where a thick crust and mantle lithosphere exist (e.g. Delph et al., 2017; Portner et al., 2018). Also, the concomitance of uplift in the modern Central Taurides and subsidence in the offshore Outer Cilicia Basin (OCB) to the

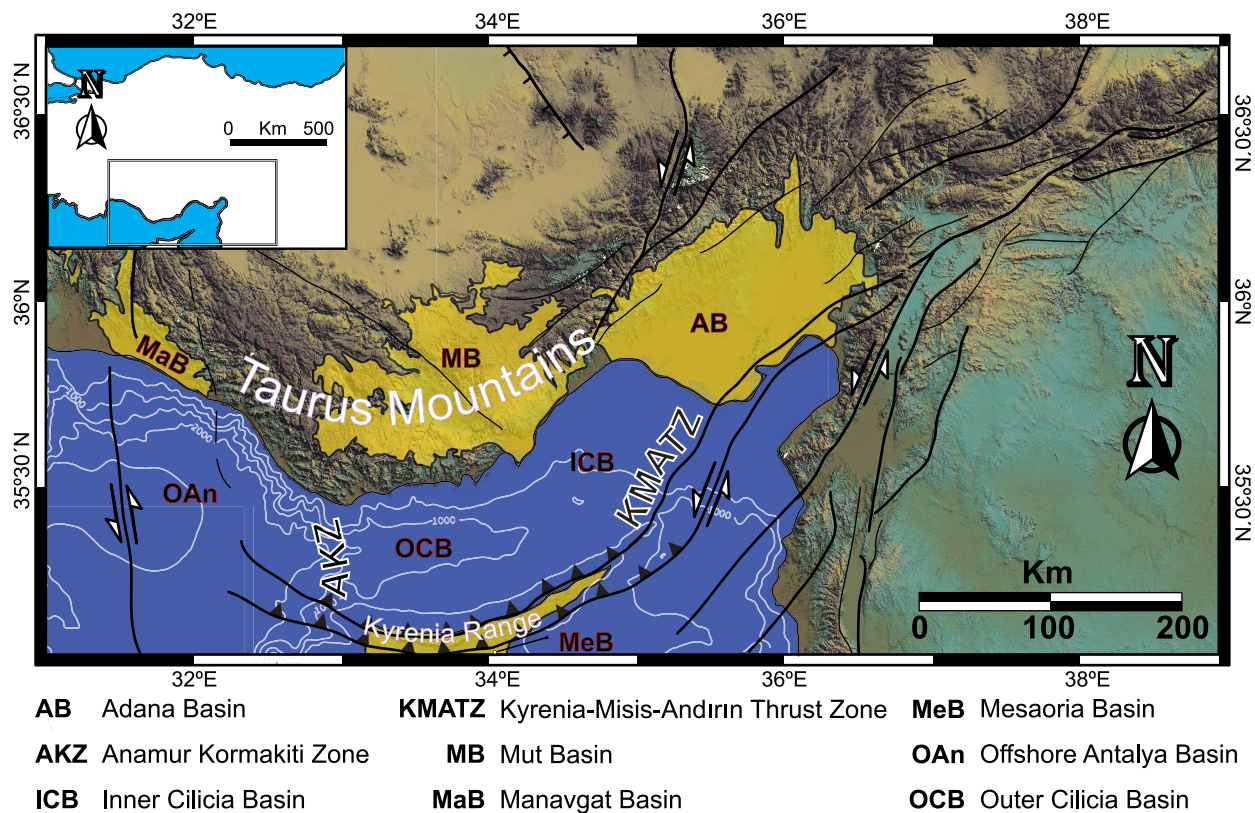


FIGURE 1 Location map, showing the main marine Miocene basins in and around the study area of this contribution (onshore basins are in yellow, offshore basins are marked by their acronyms). The structures depicted in this map are based on the analysis of 1-arc DEM and LandSat 7 images from NASA. We depict the motion of the structures as known in the available literature

south (e.g. Walsh-Kennedy et al., 2014) indicate short-wavelength vertical motions in the long-term, at odds with the long-wavelength vertical motions expected during asthenospheric upwelling (e.g. Göğüş & Pysklywec, 2008). Stable isotope paleoaltimetry estimates suggest that 2 km of relief existed at 5 Ma (Meijers et al., 2018), a finding also at odds with models proposing epeirogenic uplift. Finally, compressional tectonics of the Cyprian subduction zone is attested by tapering-southward forearc basins atop south-verging thrust systems in the offshore (e.g. Aksu, Calon, Hall, Mansfield, & Yaşar, 2005; Aksu, Calon, Hall, & Yaşar, 2005; Calon, Aksu, & Hall, 2005a; Calon, Aksu, & Hall, 2005b; Hall, Aksu, Calon, & Yaşar, 2005; Hall, Calon, Aksu, & Meade, 2005), in the Kyrenia Range, and in the Messaoria Basin (e.g. McCay, 2010; McCay & Robertson, 2012; McCay et al., 2012). These observations provide a different frame whereby the southern margin of the Central Anatolian Plateau may have been uplifted ‘actively’ by contraction within the Cyprus subduction system.

Here, we apply a multi-scale approach and consider the SCAP within the larger context of subduction in the Central Cyprus Arc. We analyse key fieldwork observations in the Mut Basin, lying atop the Tauride Mountains to the north and interpret and depth-convert N-S trending seismic lines in the offshore Outer Cilicia Basin (OCB) (Figure 1). We link these basins in regional onshore-offshore cross-sections to delineate a monocline at plateau margin scale that we analyse geometrically. Integrating this with our data along the Central Cyprus forearc, we evaluate

the time of formation of the plateau margin, and discuss its growth mechanism, tectonic setting and potential geodynamic drivers.

2 | BACKGROUND

A broad Miocene subsidence initiated marine deposition and led to a wide basin in the NE Mediterranean (e.g. Walsh-Kennedy et al., 2014). This regional event allows for correlations across onshore and offshore sites regionally in our region of study (Figure 2). Whereas subsidence continued until present in the Cilicia Basin (in the centre of the marine basin), the basin was disrupted by uplift in the Central Taurides (to the north) (e.g. Cosentino et al., 2012), in the Kyrenia Range, and to the south (e.g. Calon et al., 2005a) (Figure 3). Such vertical motions exceed glacio-eustatic signals described for the area (e.g. Bassant, Buchem, Strasser,

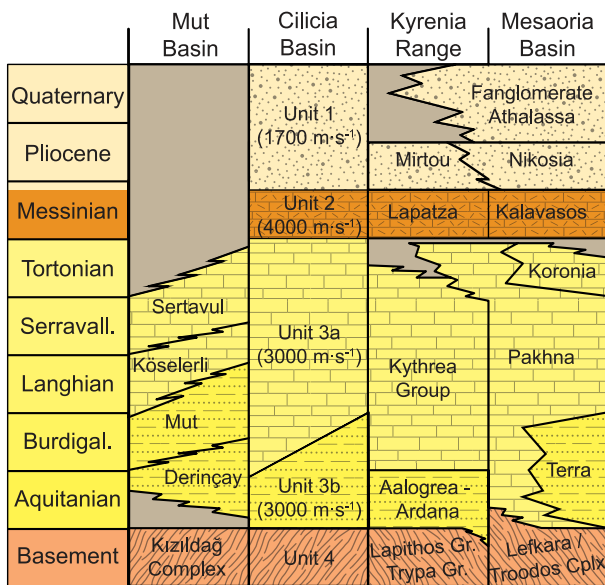


FIGURE 2 Seismic stratigraphy of the Cilicia Basin, showing the correlations between seismic stratigraphic units and the onland sedimentary successions and exploration wells. Modified following Aksu, Calon, Hall, Mansfield et al. (2005) and Calon et al. (2005b), and updated after Cosentino et al. (2013), Faranda et al., (2013)

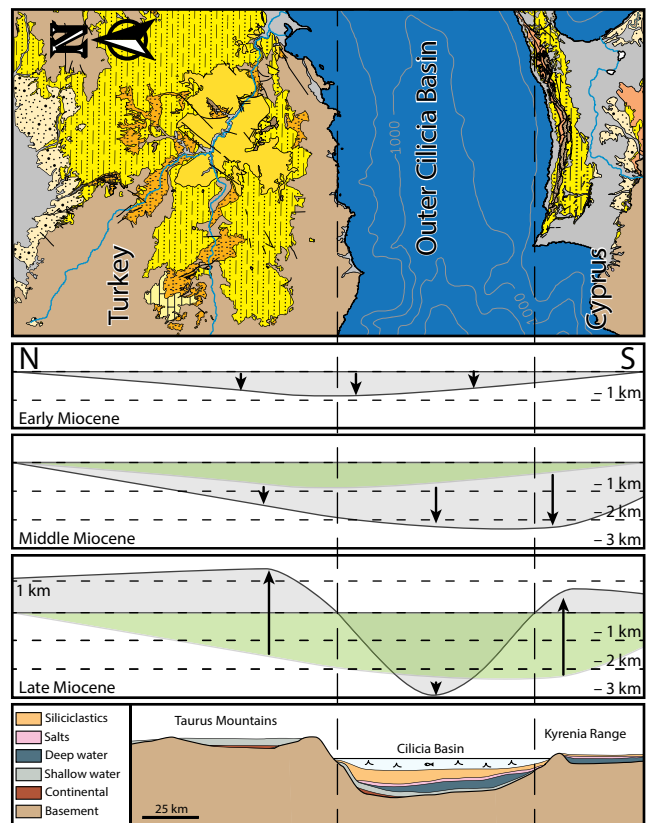


FIGURE 3 Schematic section showing first order vertical motions along the study area and their overall scale. The vertical scale is estimated as an approximation to the depth of deposition. The black line represents the position of the basement at every time-step, and the green area shows the location of the basement in the previous time-step. Arrows depict the relative vertical displacement between previous and succeeding time-steps. At the bottom, a schematic N-S regional cross section across study area (approx. from Karaman to Nicosia), shows the main type of depositional environment. Vertical exagg. 2.5

& Görür, 2005; Janson et al., 2010; Cipollari, Halásová, Gürbüz, & Cosentino, 2013) and should be regarded as portraying two different tectonic events, i.e. protracted regional subsidence since the Early Miocene, and Late Miocene differential motions (Figure 3).

The broad subsidence changed Late Oligocene-Early Miocene continental deposition in Anatolia and surrounding regions (e.g. Yetiş, Kelling, Gökçen, & Baroz, 1995; Clark & Robertson, 2002, 2005) to marine deposition (e.g. Robertson, 1998; Bassant et al., 2005; Eriş, Bassant, & Ülgen, 2005; Şafak, Kelling, Gökçen, & Gürbüz, 2005). Continued subsidence resulted in a broad marine basin (e.g. Walsh-Kennedy et al., 2014) that covered south Turkey (Çiner, Karabiyikoğlu, Monod, Deynoux, & Tuzcu, 2008; Karabiyikoğlu et al., 2000) (Figure 1) and an extensive area further south (Aksu, Calon, Hall, Mansfield et al., 2005; Aksu, Calon, Hall, & Yaşar, 2005; Hall et al., 2005; Burton-Ferguson, Aksu, Calon, & Hall, 2005; İşler, Aksu, Hall, Calon, & Yaşar, 2005). In the vicinity of the Kyrenia Range, deposition of the mostly deep-water upper Oligocene to upper Miocene sequence preceded shallow deposits, broadly similar to basins to the north and north-east, and with a common Tauride source (McCay & Robertson, 2012).

Surface uplift to the north exposes on top of the Central Taurides a sedimentary sequence of >1 km (Şafak et al., 2005) of the preceding Miocene basin. The top of this sequence is uplifted by 2 km and dated as 8 Ma, Late Tortonian (Cosentino et al., 2012), whereas younger rocks outcrop in paleo-valleys and areas near the coast (Öğretmen et al., 2018). In the offshore to the south, the base of the Messinian reaches 2 km depth in the Outer Cilicia Basin (OCB) (Aksu, Calon, Hall, Mansfield et al., 2005). Farther south, sedimentary deposits belonging to the preceding Miocene basin now outcrop in the Kyrenia Ridge (Calon et al., 2005b; McCay et al., 2012) (Figure 3). While south-verging contractional structures accommodate these vertical motions in the Kyrenia Range and further south, no regional upper-crustal structures are known to accommodate uplift in the Central Taurides.

2.1 | Northern onshore domain: Central Taurides and Mut Basin

The E-W south-arched Central Taurides outcrop in the northern onshore domain, to the north of the OCB (Figure 1). Lower to Upper Miocene sediments, mostly marine, were deposited atop the pre-Miocene Tauride basement (e.g. Monod, 1977; Andrew & Robertson, 2002; Bassant et al., 2005; Eriş et al., 2005) and then uplifted (Figure 3). These marine sediments belong to the Mut Basin and are coeval with fluvio-lacustrine deposits known from seismics for the Tuz Gölü area farther north (Fernández-Blanco,

Bertotti, & Çiner, 2013; Görür, Oktay, Seymen, & Sengör, 1984; Huvaz, 2009). Rocks in both the areas are in turn unconformably covered by terrace and alluvial fan Pliocene to Quaternary continental deposits (Monod, Kuzucuoğlu, & Okay, 2006; Özsayin et al., 2013) (Figure 4 - section a). Miocene rocks in the southern margin of the Mut Basin may shape a monocline on top of the basement, with a roughly flat surface in the hinterland that progresses into gently south-dipping geometries in its southward offshore continuation (Figure 4 - section b; Fig. 22 in Çiner et al., 2008). Such upwarp flexure at the scale of the Central Taurides cannot be accommodated by syn-depositional faulting leading to small-scale intrabasinal ridges and depressions (e.g. Ilgar & Nemeç, 2005).

2.2 | Offshore domain: Outer Cilicia Basin

The Outer Cilicia Basin (OCB) lies in the offshore domain between the mainland areas of south Turkey and north Cyprus (Figures 1 and 4). The OCB is an 160 km E-W elongated basin with a N-S extent of 120 km (Figure 1). The OCB sea floor has a concave shape that opens and deepens from 800 to 1,100 m westwards, and shallows gradually eastwards into the less in-filled basin sectors of Inner Cilicia and Adana (Aksu, Calon, Hall, Mansfield et al., 2005; Evans, Morgan, Evans, Evans, & Woodside, 1978). The Cilicia-Adana basin complex is bounded to the south and southeast by the arcuate culmination of the south-verging Kyrenia-Misis-Andırın Thrust Zone (Figure 1). The culmination of these imbricate thrusts embays sediments with east and northeast sources (Evans et al., 1978; McCay, 2010), and results in the asymmetrical deposition of thick Miocene and younger sediment infill of the basin complex (e.g., Aksu et al., 2014), as well as its relatively flat and markedly shallow basin floor (Figure 3). To the west, the OCB sea floor deepens 1 km in a horizontal distance of 50 km, towards the Antalya Basin.

2.3 | Southern onshore domain: Kyrenia Range and Messaoria Basin

Bounding the OCB to the south is the E-W trending Kyrenia Range and further south, the Messaoria plain (Figure 4). The Kyrenia Range outcrops as a deep-rooted imbricate thrust system that verges south (Calon et al., 2005a, 2005b) setting basement and Miocene rocks atop Pliocene and being in turn covered by Pleistocene rocks (Calon et al., 2005b; McCay & Robertson, 2012) (Figure 4 - section c). Southwards, the Messaoria Basin is a wedge-top Paleocene to Recent asymmetric basin (McCay, 2010) (Figure 4 - section d). Further south, compressional focal mechanisms are recorded along the Cyprus Arc trench (Imprescia, Pondrelli, Vannucci, & Gresta, 2012).

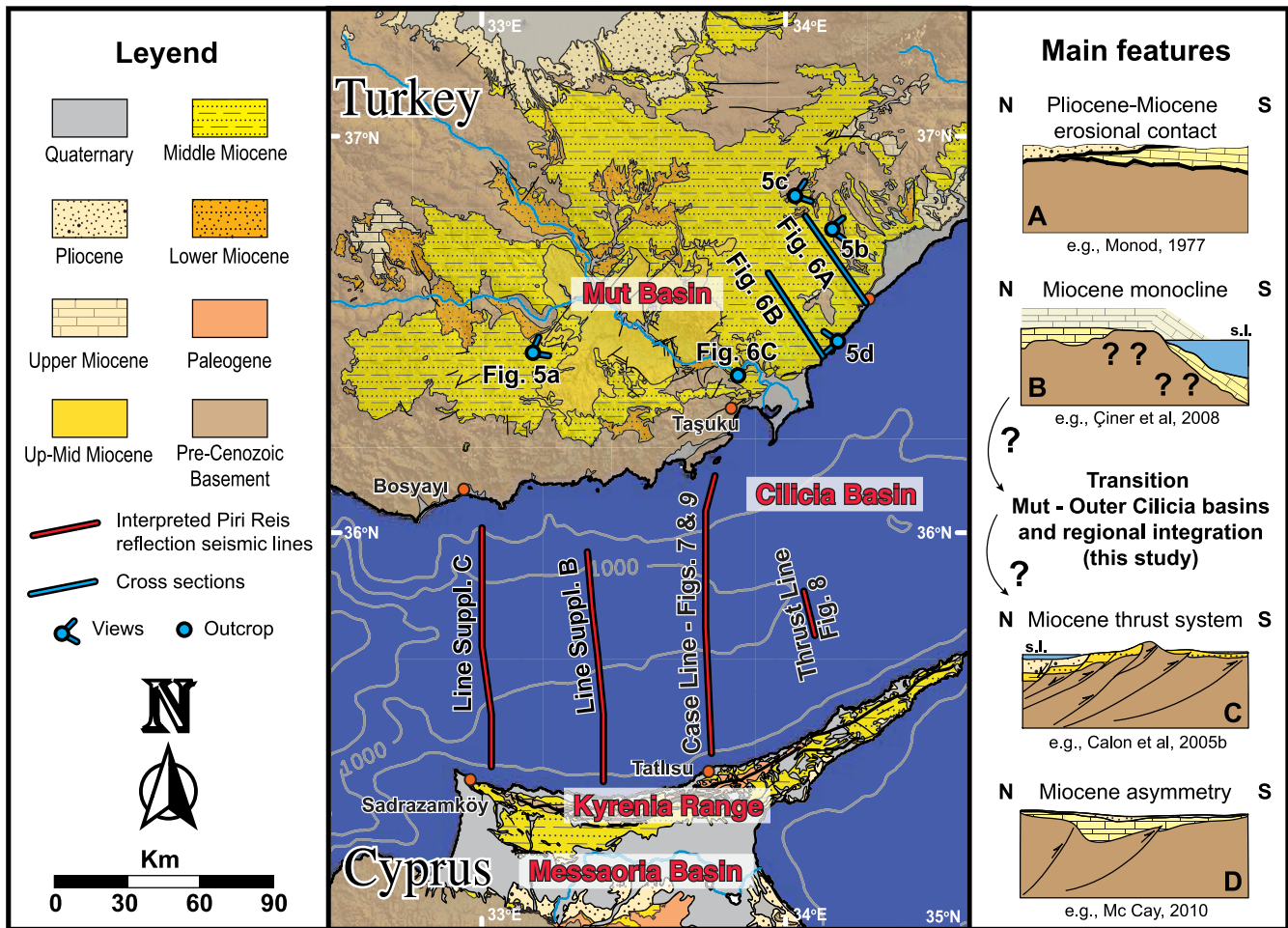


FIGURE 4 Map showing the different tectono-stratigraphic components in and around the study area. The geological map of South Turkey and Center-North Cyprus depicts a common age nomenclature for the Cenozoic units. The age integration is based on the ages shown for the MTA Geologic Map of Turkey 1:500.000, the Geological Map of Cyprus 1:250.000, and the stratigraphic correlation shown in Figure 4. The map shows also the location of some figures of this contribution. On the right hand, the main geometric and contact relationships for the area and one representative study for each of them are shown

3 | NORTHERN ONSHORE DOMAIN: CENTRAL TAURIDES AND MUT BASIN

We conducted fieldwork in the Ermenek and Mut basins to study gently-deformed Miocene limestones of mostly shallow marine origin lying atop the modern Central Taurides. We aimed at: (a) determining the geometry of the basement-Miocene contact, (b) identifying regional scale accommodation structures potentially contributing to the vertical movements and (c) assessing the regional stress field during the motions.

3.1 | Monocline flexure in Miocene rocks

The Miocene rocks lie unconformably on, and in a parallel dip-slope to, the erosional surface that truncates the basement layers at high angles (Figure 5a,b,d). The Miocene

succession overlies entirely pre-Miocene paleotopography of a few hundred metres (Figure 5a,b), against which local onlaps are common (Figure 5c). When not eroded, the lateral continuity of the Miocene dip-slope is remarkable throughout the basin, implying that pre-Miocene paleotopography was fully covered by the Late Miocene. The Miocene dip-slope is best exposed in N-S and NW-SE steeply incised valleys, i.e. the Göksu River and rivers north of Erdemli (Figure 5a,b). In the latter rivers, the Miocene marine succession can be followed for horizontal distances of 20 km, losing elevation from 1,600 to 400 m (slopes of 3%) (Figure 5b). While the succession gently gains elevation further north (Figure 5a), these rocks are often eroded in coastal areas southwards (Figure 4).

The Miocene rocks form a monoclinial flexure at the scale of the entire basin (>100 km, Figure 5a). Along strike, the monocline has an arcuate geometry at the regional scale that follows to a large extent the modern coastline of south Turkey. The broad

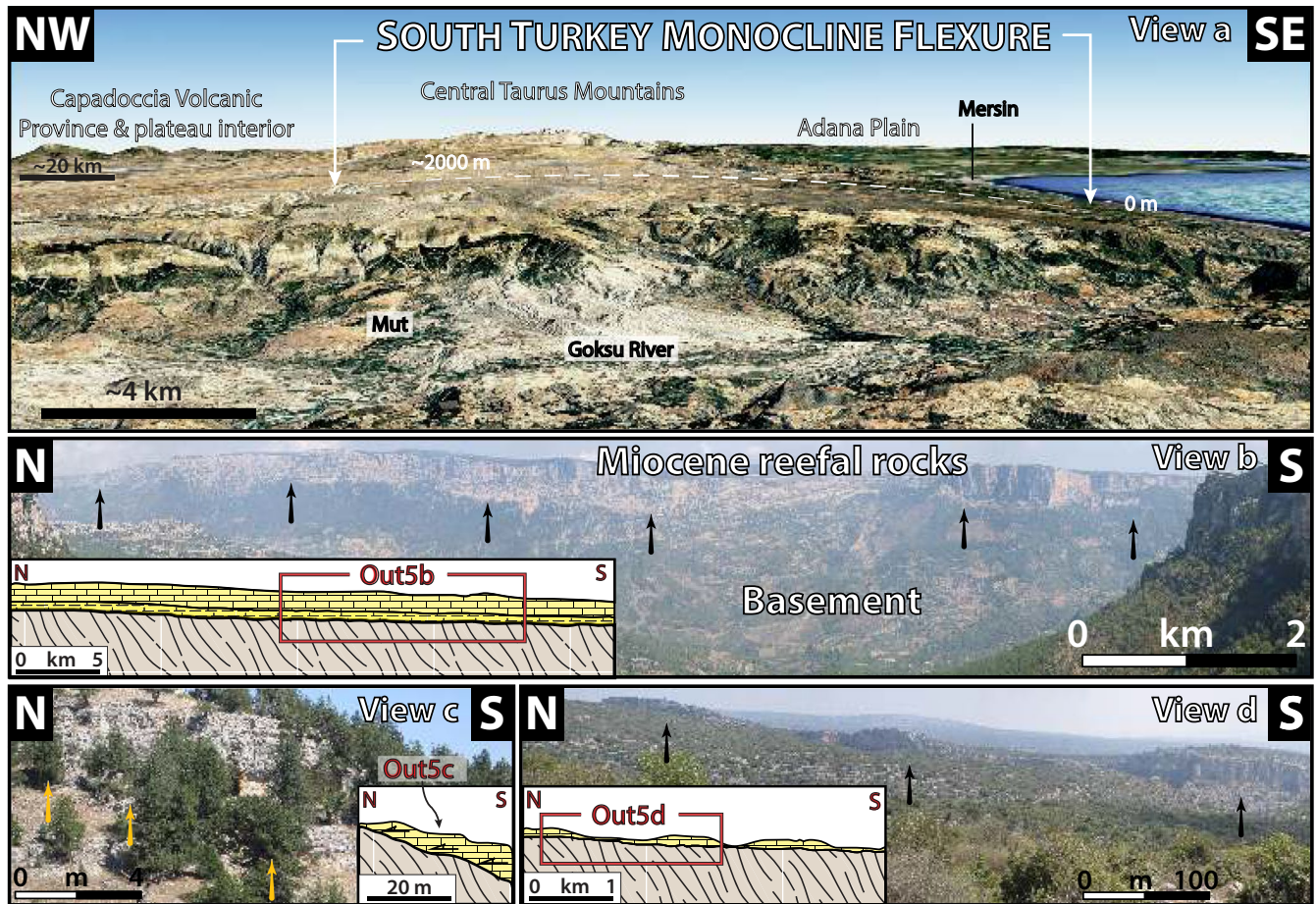


FIGURE 5 (a) GoogleEarth oblique 3-D view of the Miocene monocline flexure at the scale of the whole Mut Basin, looking NE. The Göksu Gorge is in the middle-ground and the Cappadocia Volcanic Province and the Central Anatolian Plateau interior is in the background. (b, c, d) Different views of the contact relationship between Miocene rocks atop basement rocks in the Mut Basin, roughly along latitude. Arrows mark the contact between the basement (below) and the infill (above). Basement-infill contact relationships are dependent on the scale of observation; deep-slope at the basin scale (b) yet locally onlapping (c)

hinge of the monocline lies at 40 km from the coast in the basin centre and 30 km away from it eastwards. Across-strike, the inland limb is sub-horizontal, with overall dips ranging from horizontal to 10° seaward and transitions southwards to the steeper limb, with 8° to 20° dips seaward (Figure 5a). Regionally, dip angles of 10° dominate. Transitions both along and across the strike of the monocline are smooth. In brief, a regional-scale Miocene monoclinial flexure that dips gently southward transitions from the elevated topography of the Central Anatolian Plateau interior to the Mediterranean Sea (Figure 5a).

3.2 | Other large-scale observations

Large-scale observations are consistent with regional contraction. Erosive terminations of the basin to east and west are parallel to basement ridges that outcrop in arched-south orientations parallel to the coast (ENE-WSW in the east of the Mut Basin, and E-W in the west) (Figures 4 and 5). Miocene rocks predominantly strike parallel and dip perpendicular to

the outcropping basement ridges they bound at present. This indicates that both pre-Miocene basement and Late Miocene rocks deform together after deposition of the Miocene rocks. Further, smaller folds with km-scale wavelengths form across-strike of the regional monocline. Folds are best observed to the SE of the Mut Basin along NW-SE geological cross-sections that run across the regional monocline axis and reach the coast (Figure 6). Cross-sections in Figure 6 have the best spatial coverage of bed attitude data of Middle Miocene immediately on top of the basement and depict the folds as gently asymmetrical with south-dipping flanks steeper than north-dipping ones. These observations agree with the regional monoclinial flexure of the modern Central Taurides.

3.3 | Outcrop-scale observations

Syn-sedimentary outcrop-scale structures are scarce in the Miocene rocks of the Mut Basin. Figure 6 (bottom) shows several reverse faults in Middle Miocene limestones on a

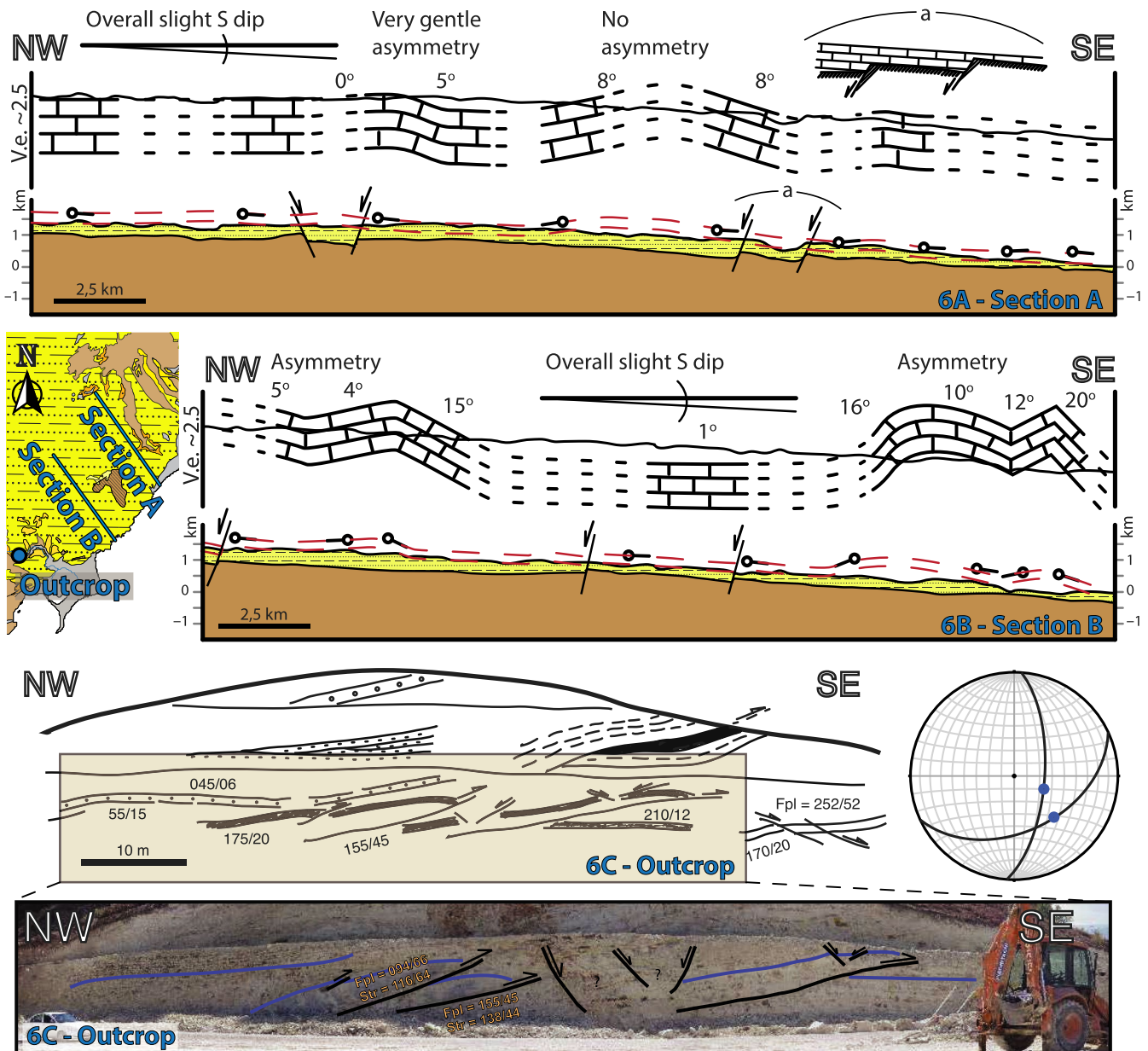


FIGURE 6 Cross-sections and reverse faults in the Mut Basin. The upper two panels show the geometries of the Miocene deposits and their relationships with basement. For each transect, the lower section corresponds to a 1:1 cross section representing the geometry of the first layer deposited on top of the basement, and the upper section represents a vertically exaggerated simplification of the Miocene and main geometries as well as representative field measurements. The depth of the basement is located on the basis of Bassant et al. (2005) and field observations. The lower panel shows reverse faults in a mid-Miocene outcrop. The upper image is a hand-drawn overview of the main structures seen in the outcrop and some representative in-place measurements. The lower image shows the interpretation drawn on top of a picture. On-site indications of relevant bed and fault attitude, and striae data are also shown

road-cut <10 km from the coast. Motion of internally coherent rock packages along faults with planar attitudes, resulting in fault-propagation fold ‘heads’ at southerly positions, discounts formation by slumping in soft sediments. These reverse faults verge roughly to the SE and show striae on two fault planes that indicate a NW–SE motion (Figure 6, bottom) and are immediately covered by inclined undeformed layers, thus characterising shortening during the Middle Miocene.

4 | OFFSHORE DOMAIN: OUTER CILICIA BASIN

Seismic profiles in the area were obtained in 1991 and 1992 by the Memorial University of Newfoundland, in collaboration with the Institute of Marine Sciences and Technology, Dokuz Eylül University. We present here three N-S multichannel reflection profiles (Figure 7 and Supporting

Information Appendices S2 and S3; location in Figure 4), and an inset of a fourth line (Figure 8). The three N-S seismic profiles, between 70 km and 100 km long, are 30–35 km apart from each other in the east-west direction. Together, the seismic lines cover an area south of Turkish onland locations Bozyayı and Taşuku, and reach close to Sadrazamköy and Tatlısu towns on the Cyprus north coast (Figure 4). All three seismic profiles are consistent laterally and show only limited variations across the OCB axis. Therefore, we describe below the eastern line and use it as representative for the OCB as a whole (Case Line; Figure 7). We refer to the other two profiles (Supporting Information Appendices S2 and S3) in the text as needed. We use the GeoSuite AllWorks® software to transform seismic profiles images in .pdf format to seismic data format (SEG-Y), and convert to true-depth to obtain the resulting interpreted seismic lines.

We use the regional correlation of Aksu, Calon, Hall, Mansfield et al. (2005) (see their Figure 6) to constrain the age of the seismic units in the Cilicia-Adana basin complex, based on stratigraphic compilations from previous

studies and bio-/lithostratigraphic data on exploration wells by the Turkish Petroleum Corporation (Aksu, Calon, Hall, Mansfield et al., 2005; Calon et al., 2005b) (Figure 1). This correlation is here updated on the basis of Cosentino et al. (2013) and Faranda et al. (2013) (Figure 2). Supporting Information Appendix S1 provides a succinct description of the seismic facies that are exhaustively described in Aksu et al. (2014).

We interpreted the seismic profiles by means of seismic facies. Characteristic packages of reflections allow the distinction of four seismo-stratigraphic units (second row in Figure 7 and in Supporting Information Appendices S2 and S3) that correspond to those originally defined by Aksu, Calon, Hall, Mansfield et al. (2005) for the area. We traced the most continuous reflections in the depth-converted lines and analysed the modern geometry, unit thicknesses, contact relationships and syntectonic growth of all three seismic profiles (third row in Figure 7 and in Supporting Information Appendices S2 and S3). We applied the seismic velocities in Figure 2 to each seismic unit

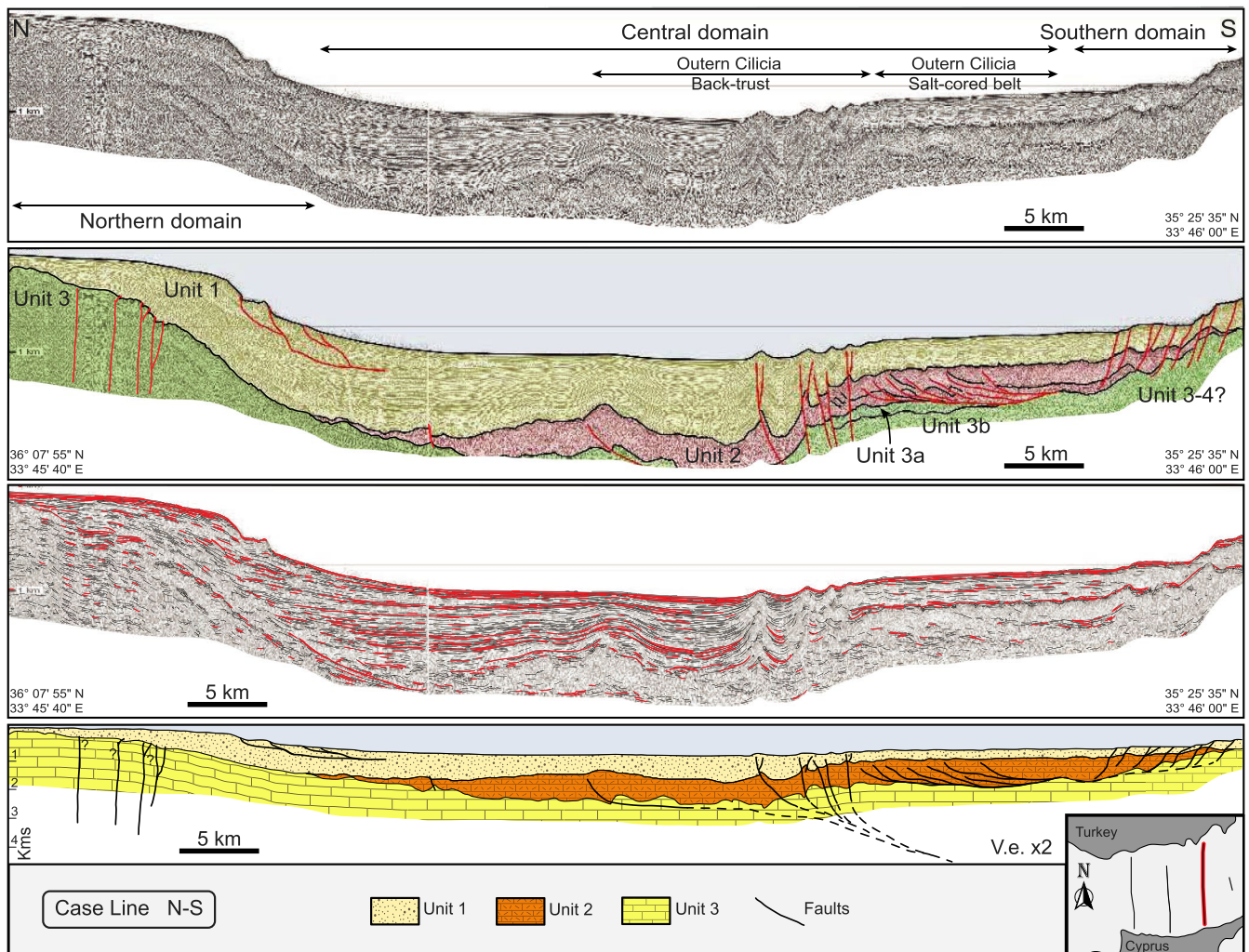


FIGURE 7 Original, interpreted in two-way-traveltime (TWT), traced with reflections in TWT, and depth-converted profile Case Line

for time-to-depth conversion of the seismic profiles (fourth row in Figure 7 and in Supporting Information Appendices S2 and S3).

4.1 | Contact relationships and thickness variations

In the northern end of the Case Seismic Line, the reflections of Unit 1 (latest Messinian - Recent) onlap the erosional surface bounding the pre-Messinian Miocene unit (Figure 7). Southwards, Unit 1 reflections dip basinward and seismic packages show increasing thickness in this direction (from 200 m to 750 m in approx. 15 km). Immediately south of the Turkish shelf break, Unit 1 shows a broad depocentre (25 km) with thicknesses of >850 m. Depocentre thicknesses are maximum to the north and related to a series of S-dipping normal faults that offset the sea floor and merge at a horizontal level 1,000 m below sea level. Thicknesses decrease to 550 m within the central-southern area of the depocentre due to a pop-up structure in Unit 2, formed by a south-dipping thrust fault, and leading to syntectonic wedging out of the Unit 1 reflections northward. To the south of the depocentre, Unit 1 thins to 350 m and its base shallows in less than 5 km from depths of 1,900 to 1,200 m. Constant thicknesses of 300–350 m exist further south, except close to the continental shelf of north Cyprus, where Unit 1 thins, partially due to the extensional offsets of a north dipping fault system.

Unit 2 pinches out from the centre of the Case Seismic Line and shows a southward step-up sigmoidal shape, by which the same reflections are found at shallower positions to the south (Figure 7). A prominent deep-rooted system of steep north-verging thrusts controls the sigmoidal shape of Unit 2 and the elevated position of the southern basin sector of the basin relative to the northern one. Immediately south of the steep deep-rooted thrusts, a smaller set of thrust faults dip gently southward. This second system is rooted in the base of Unit 2 and creates salt-cored anticlines that repeat the sequence and thicken Unit 2 up to maximum thicknesses of 700–750 m. Unit 2 thins away from its depocentre both to the north and south in horizontal distances of <10 km.

Unit 3 has no evident terminations in the Case Line and its base cannot be distinguished and thus, no thickness determination was possible. At the northern end of the Case Line, an erosional unconformity below Unit 1 (latest Messinian-Recent) forms the top of Unit 3 (pre-Messinian Miocene) (Figure 7). To the south, the unconformity fades and Unit 3 underlies the Messinian evaporites of Unit 2. Further south, the top surface of Unit 3 steps upward in the same direction and marks an offset in relation to the deep-rooted thrust system. At the southernmost end of the line, an erosional unconformity again sets the top of Unit 3.

4.2 | Structural domains

A sea floor step divides the Outer Cilicia Basin (OCB) in two around its centre in relation to a deep-rooted thrust system observed in all seismic lines (Section 4.2.1; Figures 7 and 8, Supporting Information Appendices S2 and S3). Sea bottom depths are visibly shallower on the southern side than on the northern side of the basin, correlating with two structural domains trending E-W (Figures 7 and 8, Supporting Information Appendices S2 and S3), the northern (Section 4.2.2) and southern sub-basins (Section 4.2.3).

4.2.1 | Central Outer Cilicia Basin main thrust

The Central OCB main thrust (Figure 8) is a top-to-the-north deep-rooted thrust fault system that bounds the northern and southern OCB sub-basins, leading to prominent syntectonic wedges (Figure 7, Supporting Information Appendices S2 and S3). Around 20 km farther east than the Case Line, the seismic reflection image with higher resolution (from the 2008 seismic campaign) (Figure 8) illustrates the main thrust tip and the change in seafloor bathymetry at 1 km water depth. Westwards, the Central OCB main thrust changes from a single fault (Figure 8) to several thrusts (Figure 9e). Thrusts offset both the M- (up to 100 m) and the N- reflectors, and are only partially influenced by diapirism, as shown by several ramp anticlines underneath (Figures 7 and 9e). The tips of these E-W trending thrusts are evidenced by reverse offsets, northward step-down of unit boundaries, and Unit 1 reflections, as well as the sea floor bulges (Figure 9e). The frontal and second sliver thrust tips are expressed as bulges in the seafloor in all three lines, within a concave area 5–10 km long, while bulges located southward attenuate and eventually dim toward the east (Figure 7, Supporting Information Appendices S2 and S3).

4.2.2 | Northern Outer Cilicia Sub-Basin

The sea floor of the northern OCB sub-basin dips south very gently and deepens in a continuous manner from the Turkish break-of-slope. Unit 1 (latest Messinian - Recent) contains two fault systems in the north of the OCB (Figures 7 and 10). The youngest is an extensional fault system dipping south that reaches the sea floor of the shelf break-of-slope and soles into a single structure parallel to the reflections (Figure 7). The oldest is a series of roughly vertical faults with small offset that lie within Unit 3 (pre-Messinian Miocene) and cut the corrugated erosional surface at the base of Unit 1 (Figure 9b). The kinematic character of the latter faults is ambiguous as they are steep and their associated reflection offsets are unclear. These faults may represent the local equivalent of the

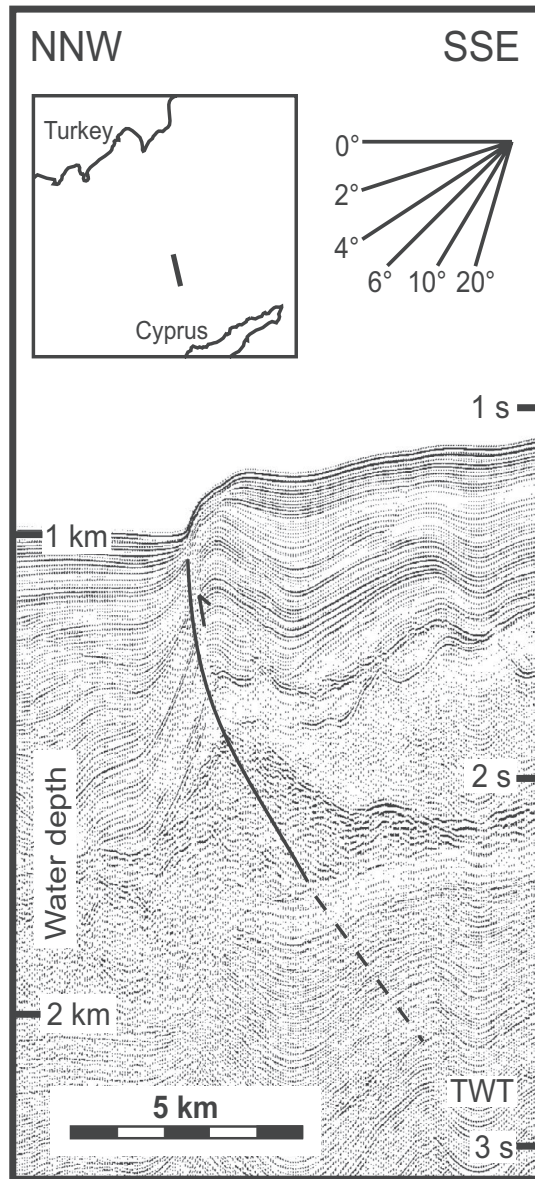


FIGURE 8 The Central OCB main thrust, as shown in a crop of a seismic reflection image to the east of the Case Line. The image shows the depth difference between northern and southern sectors of the OCB and the steepness of the thrust faults, in TWT. Source: Piri Reis Seismic Reflection Profiles (2008 campaign)

Kozan Fault Zone (Aksu et al., 2014; Bridge, Calon, Hall, & Aksu, 2005; Burton-Ferguson et al., 2005), which is mapped farther northeast as a wide transtensional fault system with sinistral offset. The total down-to-basin offset of the top of Unit 3 across the fault system is 150 m (Figures 7 and 9b). Regardless of their kinematics and significance, these faults occur in an inflexion area of the Unit 3 upper boundary, which transitions basinward from gently to distinctly south dipping (Figure 9a–c). Unit 1 (latest Messinian - Recent) reflections have a similar change in geometry, dipping gently south. Reflections onlap at low-angle the erosional surface north of the faults (Figure 9a), and lie in dip-slopes and at higher angles basinwards (Figure 9c).

4.2.3 | Southern Outer Cilicia Sub-Basin

The sea floor of the southern OCB sub-basin dips north with variable slopes, and shows a corrugated nature and a step-like bathymetry farther south. Two fault systems, one extensional and one contractional, root at the base of Unit 2 (Messinian) (Figures 7 and 9). At proximal positions, the extensional fault system transects the boundaries of Unit 1 and Unit 2 with increasing offsets southward (Figure 7). These normal faults displace the sea floor by >80 m leading to a step-like bathymetry that alternates gentle south-dipping with steep north-dipping slopes, while deepening 300 m northward in 10–15 km. Total offset increases eastward (cf. Figure 7, Supporting Information Appendices S2 and S3). Many of these normal faults vary from subvertical at the sea floor to low angle at depth and probably sole into a sub-horizontal surface. At distal positions, an imbricated system of top-to-the-north low-angle faults sole out into the base of the Messinian unit (Figures 8 and 10f). These thrusts, collectively named reflector package ‘ α ’ in Aksu, Calon, Hall, Mansfield et al. (2005), offset several reflections within Unit 2 and form a gentle syncline-anticline succession in Unit 1 without cutting the Unit 2 upper boundary (Figure 7). Here, the relatively flat sea floor gently increases from 800 m to 900 m in depth over 15–20 km northwards.

5 | ONSHORE-OFFSHORE LINKAGE ACROSS THE PLATEAU MARGIN

We recognise three structures of regional relevance: a monocline in the north, a deep-rooted thrust system in the centre, and a toe-slope system in the south. The latter two structures are controlled by the south-verging thrusts of the Kyrenia Range (Figure 9g). The first of these, the Central OCB main thrust (Figures 8 and 9e) functions as a back-thrust linked to the Kyrenian culmination, and perches on the southern half of the OCB (Supporting Information Appendix S4). The second, the toe-slope system (Figure 9f), is a gravitational kinematic response to the slope instabilities in the margin of the perched basin, aid by the mobility of the Messinian layer (Supporting Information Appendix S5). Below, we focus exclusively on the deformation and sedimentary patterns resulting from the growth of the third structure—the Miocene monocline of south Turkey. We reconstruct the monocline by coupling onshore and offshore geology across the southern margin of the Central Anatolian Plateau (SCAP). We consider the kink structure on the Turkish shelf (Figure 9a–c) as kinematically linked with the equivalent, albeit larger, monocline flexure observed in the Mut Basin (Figure 5) and apply inferences on the kinematics of the former (section below) to the latter.

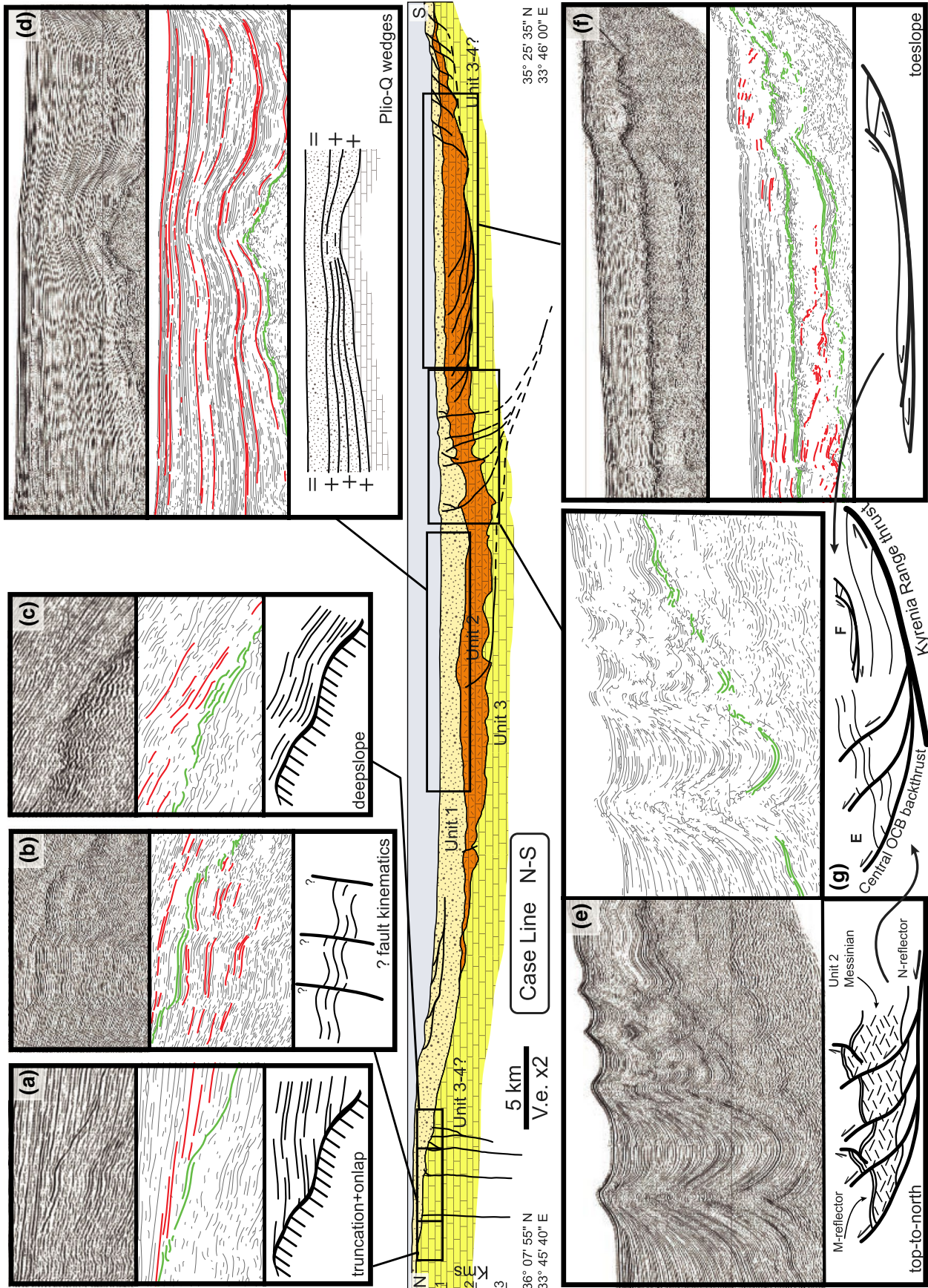


FIGURE 9 Depth-converted Case Line is shown at the centre, and used to locate the main features observed along the OCB, which are shown in the different insets. Each inset shows the seismic image in time, the seismic image with traced reflections, and the schematic representation of the observed structures and sedimentary geometries seen along the seismic lines. In the traced image, reflections within the units are shown in red and the reflections in green define boundaries between units

5.1 | Late Miocene to recent kinematics

On the upper sector of the Turkish shelf, the reflections of Unit 1 (latest Messinian - Recent) onlap the erosional contact with Unit 3 (pre-Messinian Miocene) (Figure 9a). Unit 1 reflectors progressively pass basinward to dip-slope geometries (Figure 9c), developing syntectonic wedges that open in the same direction (Figure 10). The scale of these wedges dictates that they are not the result of climatic oscillations. We distinguish different sub-units within Unit 1 and analyse the location of the transition between onlap and dip-slope reflectors. Younger sub-units have the onlap-dip slope transition at northward locations and develop

syntectonic unconformities and on-structure wedges, i.e. cover both limbs of the fold (see Patton, 2004 for terminology) (sub-units 1–4; Figure 10). This geometrical pattern suggests that a continuous increase in accommodation space alternates with abrupt decreases during fold-kink growth (Patton, 2004; Riba, 1976). Although sedimentation entering the system laterally could produce similar patterns, parallel horizontal reflections in the upper part the sequence suggests subsidence (or sea level rise). Located at the top of the seismo-stratigraphic sequence, sub-unit 5 is the first sub-unit that is not wedged, which indicates self-similar growth of the structure until close to recent times (Figure 10). Sub-unit 6 formed as a block at younger times.

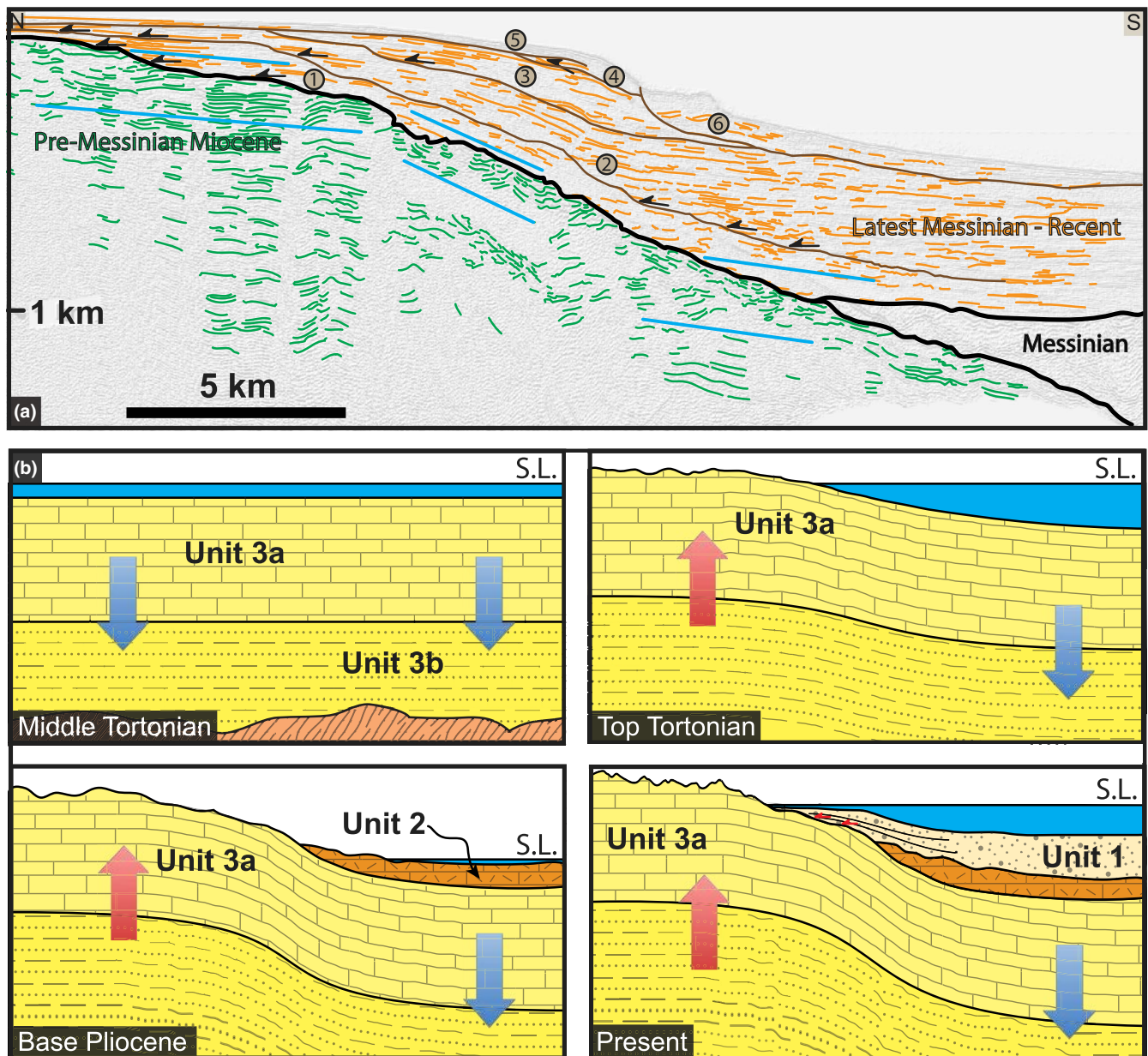


FIGURE 10 (a) Seismic image in time with traced reflections showing the angular relationships and main geometries seen in the Plio-Q and Miocene units in the South Turkish offshore. Distinct onlap-wedging characteristics allow for the differentiation of six sequential packages, numbered from oldest to youngest. Representative dips of reflections of both units are shown in blue. (b) Conceptual evolution of the south margin of the CAP, as derived from the analysis of seismic reflections in the northern boundary of the OCB

The underlying reflections of Unit 3 (pre-Messinian Miocene) are cut by the erosional surface. Roughly vertical faults transect Unit 3 reflections in the axial plane of a kink structure (Figure 9b); whereas Unit 3 reflections are subhorizontal in the northern areas and disrupted where faults offset the unit, they dip 25–30° basinward to the south (Figures 9a,c and 10). These geometrical relationships indicate that the kink monocline developed after deposition of at least part of Unit 3 (pre-Messinian Miocene), but prior to the onset of erosion.

5.2 | Geologic onshore-offshore cross-sections

We reconstruct two onshore-offshore cross-sections linking geological observations across the SCAP margin. We attempt to overcome the lack of data coverage and/or the discontinuity of Miocene rocks near the Turkish coast, using a different approach to reconstruct each of the two onshore-offshore cross-section. The transect on the SE plateau margin (Figure 11a) has the largest data coverage, i.e. the offshore seismic line reaches the closest to the coast in which Miocene rocks outcrop. However, the northward continuation of the offshore line towards the onshore meets basement rocks, and both sections are a considerable distance apart. The transect on the S plateau margin (Figure 11b) has the tightest age constraints,

i.e. accurate dating of the youngest pre-Messinian Miocene rocks onland and a good age estimate of its corresponding offshore unit (see Figure 2). However, age error bars and uncertainties are still large, and both correlatable units are a substantial distance apart. We use the transects with caution to provide first-order estimations of geometry, vertical displacement and shortening across the monocline.

The onshore-offshore transect on the SE plateau margin (Figure 11a) uses Section B in the Mut Basin (Figure 6b) as the continuation of the depth-converted Case Line (Figure 7, bottom). We use bed dips from the field and reflectors from the depth-converted Case Line (Figure 10a). Figure 12a depicts in red a ‘key bed’ to characterise the first-order geometry of the regional Miocene monocline structure on its flank. This ‘key bed’ represents a rock layer that is (a) at the lowest possible elevation above topography onshore, as a proxy to a rock layer that is slightly younger than the mid-Miocene outcropping rocks; and (b) at the highest possible elevation below the erosional surface offshore, as a proxy to a rock layer that is slightly older than Messinian. We thus consider the ‘key bed’ loosely as Tortonian. We obtain the ‘key bed’ in the onshore profile by extrapolating vertically up the bed attitude data of the first Middle Miocene appearance atop basement, and in the offshore by extrapolating vertically down reflections northwards from the contact between the erosional surface and the

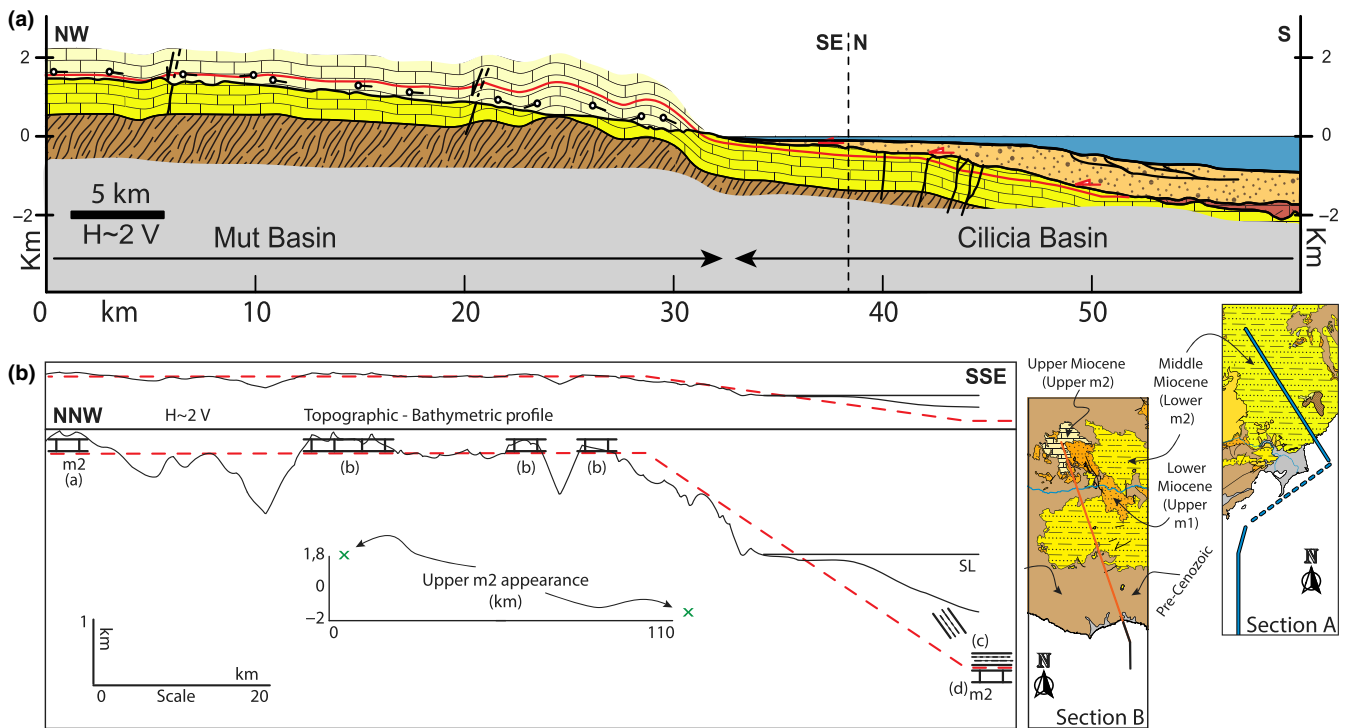


FIGURE 11 Onshore-offshore geologic cross-section in S Turkey. The red line is the ‘key layer’ and represents approximately a bed of Tortonian age. It relates with the minimum possible relative vertical displacement within the Miocene rocks that shape the monocline. (a) Onshore and offshore geometries of the Miocene deposits and their relationships with the basement. (b) Onshore and offshore link of rocks of Late Miocene age. (a) is based on Cosentino et al. (2012) and (b) is obtained from the MTA geologic maps of Adana 1:500.000 (Ulü, 2002). (c) and (d) are offshore layers obtained from the Seismic Line Supporting Information Appendix S3, and represent the base of the latest Messinian and above the Lower Tortonian, respectively.

Messinian unit. Given that the Tortonian could be at higher elevations onland and at deeper levels offshore, the steepness of the flank is a minimum estimate and thus the monocline may accommodate larger relative vertical displacement than that shown in Figure 11a.

The onshore-offshore transect on the S plateau margin (Figure 11b) has the age constraints of Cosentino et al. (2012) onshore, and Aksu, Calon, Hall, Mansfield et al. (2005) offshore. The shallow water limestones exposed onshore at the upper section of Unit 'm2' in the Geological Map of the Adana Plate [1:500,000] (Uli, 2002) are Late Tortonian, ca. 8 Ma (Cosentino et al., 2012) (a, in Figure 11b). The offshore Unit 3a, seen as fluvio-deltaics in the exploration wells, correlates with onshore formations of age base Tortonian, 11 Ma (Aksu, Calon, Hall, Mansfield et al., 2005) (d in Figure 11b; Supporting Information Appendix S3). Here, the 'key bed' that helps constrain to a first order the geometry of the monocline runs below the Upper Tortonian onland (a in Figure 11b) and above the Lower Tortonian offshore (d in Figure 11b), and is thus, again, loosely Tortonian in age. The 'key bed' transects in a horizontal line Tortonian or older rocks on land (b in Figure 11b) and either Tortonian or younger rocks offshore (c in Figure 11b represents the base of the latest Messinian). Therefore, geometrical constraints for the 'key bed' result only from restrictions by the topography near the Turkish coast that is devoid of Miocene rocks. Linking both 'm2' appearances onshore and offshore imposes a minimum boundary for the steepness of the monocline flank (Figure 11b).

We characterise a minimum-amplitude monocline geometry and infer steep Miocene beds for the monocline flank, linking onland and offland sectors with gentle south dips (Figure 11). Geometrical constraints set by the 'key bed' suggest that the monocline flank has a maximum horizontal length of 20–25 km. Similarly, the 'key bed' in both figures provides an estimate of the minimum vertical relative displacement cross the SCAP margin. Rocks depositing close to sea level show surface uplift of 1.8 km (a in Figure 11b) mirrored by 2 km of absolute subsidence (d in Figure 11b) during monocline growth. Therefore, the relative vertical displacement since the Tortonian is 3.8 km, which provides a rough average rate of vertical displacement of 0.5 mm/y. The 'key bed' allows shortening estimates of <1% across the fold structure (in 110 km for the section in Figure 11b). In our approximations to the monocline geometry, axial planes of the monocline kinks are almost parallel and seem to converge only at significant depths.

6 | DISCUSSION: MONOCLINAL GROWTH OF THE PLATEAU MARGIN IN S TURKEY

Our onshore-offshore approach allows insights on the accommodation and growth mechanics of the SCAP, provides

constraints on its time and mode of (de)formation and sets the plateau margin in the regional context of the Cyprus subduction to the south.

6.1 | Time of vertical motions

Our data suggest that vertical tectonic motions in the SCAP started >5 Ma and that relevant relief in the modern Central Taurides existed at 5 Ma. Late Miocene shallow marine rocks shaping the monocline outcrop in its uplifting sectors, and feed the thick depocentres of latest Messinian to Present sediments in its subsiding sectors (Figures 5, 7 and 11). The lateral continuity of dip-sloping Miocene rocks throughout the Mut Basin (Figure 5) implies that most of the Miocene succession deposited prior to monocline growth. Later uplift exposed the Late Miocene rocks, truncating and eroding the series (Figure 10) while subsiding sectors of the monocline continued deposition throughout the latest Messinian - Recent times (Figures 7 and 10, Supporting Information Appendices S2 and S3). Removal of substantial amounts of sediments from the rising Central Taurides since the latest Messinian (Walsh-Kennedy et al., 2014) led to a continuous stack of prominent delta lobes in the Göksu Delta (Aksu et al., 2014), and the syntectonic wedges on top of Late Miocene erosional surface (Figure 10). The above evidence is at odds with fast growth of topography after the Early Pleistocene (Schildgen et al., 2012) or the early Middle Pleistocene (Öğretmen et al., 2018). Contrarily, the continued growth since latest Miocene of the Göksu Delta and near-coast syntectonic wedges, as well as the overall low gradient stream and a wide valley floor of the Göksu River (often >30 km in width, Figures 4 and 5), are consistent with the presence of relevant (km-scale) topography in the Central Taurides before the Pliocene (Fernández-Blanco, 2014; Meijers et al., 2018).

6.2 | Accommodating structures

The flexural monocline in S Turkey is the only structure capable of accommodating the 4 km vertical gradient in Miocene rocks observed at present across the SCAP (Figure 11). The growth of the regional flexural monocline accommodates most, if not all, the counter-acting vertical motions. Concomitant vertical motions of short wavelength led to the surface uplift of S Turkey, that emerged and disconnected the Mut Basin, and to the counter-balancing subsidence of the Cilicia Basin. The present-day geometry of the monocline implies a narrow area of deformation (~20–25 km) and suggests southward strain propagation in a kink-band fashion. The fact that the axial planes of the kink-band are almost parallel between them precludes calculus of the depth of the tip of the potential fault responsible for the kink-band, and suggest that, if any such fault exists, it is likely to be located below the upper crust. Strain accumulation at depth is at variance with a potential

accommodating structure close underneath the succession, regardless of its kinematics.

Other known structures cannot accommodate the motions. Late Miocene and younger minor normal and strike-slip faulting exists in the modern Central Taurides (İlgar & Nemeç, 2005) and significant extensional and/or strike-slip faults occur to its sides (Aksu, Calon, Hall, Mansfield et al., 2005; Aksu et al., 2014). The most prominent of these fault systems, the Kozan Fault Zone (KFZ), at the south-eastern margin of the modern Central Taurides, has vertical offsets of 50–200 m in the M-reflector, and sinistral displacements of 20–35 km in the uppermost Messinian to Quaternary deposits of the Göksu Delta (Aksu et al., 2014). The amplitude of the monocline is, ad minimum, one order of magnitude larger than vertical displacements along the KFZ (Aksu et al., 2014). Moreover, transtension along the KFZ ensued during the onset of the westward motion of Aegean-Anatolia plate (Aksu et al., 2014), and thus postdates the majority of the uplift. Therefore, the KFZ potential contribution to monoclinical growth is trivial and associated strain is not related to the main geodynamic causes behind the motions discussed in this contribution. We suggest that the mechanical load of Taurides aids subsidence of its external areas, and speculate that this isostatic gradient guides the entrenchment of the KFZ between both regions.

6.3 | Tectonic regime and contextualisation

Shortening in Miocene and younger rocks record compression in south Turkey, in the offshore and along the Central Cyprus accretionary margin during growth of the southern plateau margin of Central Anatolia (Figures 6–11). In the Mut Basin, shortening is observed at several scales; Miocene infill rocks striking parallel and dipping orthogonal to basement ridges outcropping parallel to the coast (Figure 5); asymmetric Miocene folds having steeper southern flanks, and; reverse faulting during deposition of Middle Miocene rocks (Figure 6). Shortening in the Turkish shelf results in latest Miocene-Recent on-structure syntectonic wedges that open southward (Figure 10). Farther south, all other coeval regional-scale structures along the Central Cyprus margin developed by shortening (Figures 7–9 and Supporting Information Appendices S2–S5). Although monoclines grow by many different structural mechanisms (e.g. Freund, 1979; Reches, Hoexter, & Hirsch, 1981; Tindall & Davis, 1999; Willsey, Umhoefer, & Hilley, 2002; Patton, 2004), the structures described above report compressional stresses before, during and after the time of formation of the flexural monocline, and thus strongly suggest monocline growth by shortening.

Convergence between Africa/Arabia and Eurasia results in overall N-S compression between S Turkey and the Cyprus

trench. Subduction results in Miocene contraction and Plio-Quaternary strain partitioning, by which coeval thrust tectonics and left-lateral oblique stretching occur in east- and northeast-trending sectors, respectively, of the south-arched, crustal-scale thrust systems of Misis-Kyrenia Fault Zone, Amanos-Larnaka Fault Zone and the Cyprus Arc itself (e.g. Aksu, Calon, Hall, Mansfield et al., 2005; Aksu, Calon, Hall, & Yaşar, 2005; Aksu et al., 2014; Burton-Ferguson et al., 2005; Calon et al., 2005a; Calon et al., 2005b; Hall, Aksu et al., 2005; Hall, Calon et al., 2005; İşler et al., 2005). Shortening tectonics in the Outer Cilicia Basin resulted in contractional structures during the Late Miocene and the mid-Pliocene or younger times (Supporting Information Appendices S2 - S5), while transtension is clear in the southeastern sectors of the Turkish shelf and eastwards (Aksu et al., 2014). Our field evidence for the Central Taurides suggest that (a) the monocline has a south-arched geometry that follows roughly the coast; (b) shortening might have initiated as early as Middle Miocene (Figure 6) and; (c) joint deformation of pre-Miocene basement and Late Miocene rocks occurred during post-Miocene times (Figure 5; section 3.2). For similar and younger time frames, other studies report normal and strike-slip faults (İlgar & Nemeç, 2005). Taken together, we infer that the evolution of S Turkey is comparable to that of arc-parallel regional structures farther south. Similar to these regional-scale structures albeit devoid of regional ground-breaking faults, in the Central Taurides, subduction-related shortening coexists with, and may be partially overprinted by, extrusion-related transtensional structures since latest Messinian.

Shortening and uplift in the SCAP led by protracted contraction along the Central Cyprus continental margin contextualise the plateau margin as the forearc high of the Central Cyprus forearc basin system (Figure 12). Although the Central Cyprus continental margin has varied in space and time, shortening leading to the growth of structural highs and associated south-tapering forearc basins south of Turkey has been occurring since the slab retreated to close to its present position at 25 My (Robertson, 1998). The trench lies at present south of Cyprus, between the Eratosthenes Seamount and the Troodos ophiolite (Robertson, 1998). Northwards, thrusting along the Kyrenian culmination formed the Kyrenia Range, and its southwards emplacement led to the Messaoria Basin (Calon et al., 2005a, 2005b; McCay, 2010). They are the trench-slope break and a wedge-top basin. Further north along the margin, the OCB and the Mut Basin are the residual and intramassif forearc basins fragmented by the Central Taurides forearc high (Figure 12). Mio-Pliocene north-verging thrusts north of the Central Taurides (Gürer, 2017) may function as antithetic structures to the monocline, suggesting forearc high uplift as a wide anticlinorium during contraction and crustal thickening below the modern Central Taurides. Farther north, the volcanic

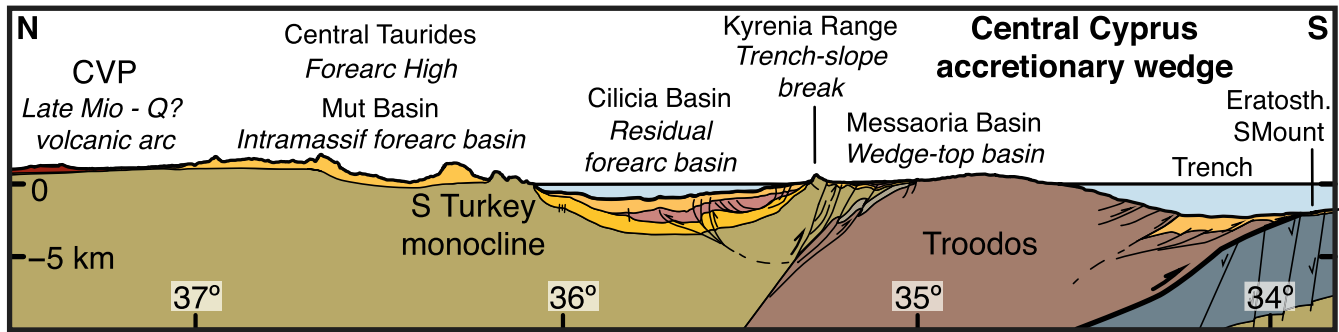


FIGURE 12 Transect across the Central Cyprus accretionary wedge (at $\sim 33^{\circ}30'E$). The transect shows the correlation between the main tectonostratigraphic features of the Central Cyprus margin and elements of a 'standard' accretionary margin with forearc high. Slightly modified from Fernández-Blanco, (2014)

arc of Cappadocia has calc-alkaline magmas with clear subduction signals since 13 Ma (e.g. Aydar, 1998) with younger magmas at southwestward locations increasing in within-plate character since 6–7 Ma (e.g. Deniel, Aydar, & Gourgaud, 1998). Although the latter has been linked to asthenospheric sources (e.g. Göğüş et al., 2017), heterogeneous lithospheric sources are deduced from penecontemporaneous Quaternary magma suites with calc-alkaline/alkaline affinities (Dogan-Kulahci et al., 2018).

6.4 | Mode of plateau margin growth

Monoclinical flexure during growth of the plateau margin before the Pliocene agrees well with paleoaltimetry estimations of 2 km of relief at 5 Ma (Meijers et al., 2018) and the subsidence signal thereafter (Walsh-Kennedy et al., 2014). Contraction at depth, crustal thickening and monocline growth are also compatible with the presence of the Central Cyprus slab, and the thick crust below the modern Central Taurides relative to the Central Anatolia Plateau interior (e.g. Bakırcı et al., 2012; Abgarmi et al., 2017; Delph et al., 2017; Portner et al., 2018). By contrast, alternative models proposing plateau margin uplift by shallow slab break-off during a multi-phase evolution (Cosentino et al., 2012; Öğretmen et al., 2018; Schildgen et al., 2014, 2012) are inconsistent with the aforementioned research. In brief, evidence shown here puts into question 'passive' isostatic uplift models for the southern margin of the Central Anatolian Plateau and points instead to 'active' contractional margin growth.

We suggest plateau margin growth by plate thickening and strain accumulation at depth, as led by thermal weakening and viscous flow in the lower crust (Fernandez-Blanco, Bertotti, Cassola, & Willett, 2012; Fuller, Willett, & Brandon, 2006). Thermally-activated viscous flow and ductile strain at deeper sectors of orogenic subduction wedges may explain advanced stages of evolution in forearcs and the development of forearc highs (Fuller et al., 2006; Pavlis & Bruhn, 1983; Pope & Willett, 1998; Willett & Schlunegger, 2010).

Applied to the southern margin of the Central Anatolian Plateau, this mechanism would imply that protracted thickening by sedimentary accretion from the Central Cyprus margin thermally activates low-strength viscous flow at the base of the Anatolian crust, and sustains the growth of the SCAP as a regional flexure at plateau margin scale.

7 | CONCLUSION

Geological evidence across the southern margin of the Central Anatolian Plateau and farther south suggest that the plateau margin developed prior to the Pliocene by shortening led by Eurasia-Africa compression. Accounting for the location, attitude and timing of first-order structures in the onshore, as well as the kinematics, tectonic regime and age of regional accommodating structures in the offshore, we infer a flexural monocline in Miocene rocks at the scale of the plateau margin. Monocline growth during post-Miocene times can explain surface uplift in the Mut Basin and its regional coupling with concomitant, short wavelength subsidence in the Cilicia Basin. We characterise the monocline as a regional kink-band fold where two gently south-dipping domains are separated by a narrow flank of 20–25 km. The Miocene rocks have relative vertical displacement rates of ca. 0.5 mm/year and shortening <1% (in 110 km). Miocene monocline wavelength and geometry are indicative of plateau margin growth in relation to deep-sourced deformation, that we understand in the context of upper crustal flexure during the development of the forearc high of the Cyprus subduction system.

ACKNOWLEDGEMENTS

The authors would like to thank the masterful editorial management of Atle Rotevatn, and the reviews by Gilles Brocard, Enrico Tavarnelli and two anonymous colleagues.

We thank the Netherlands Organisation for Scientific Research (NWO) for funding this study, part of the Vertical Anatolian Movement Project (VAMP), an ESF EuroCORE TOPOEurope. DFB is deeply thankful to Fabrizio Pepe, who provided and helped with the GeoSuite AllWorks software. Contributions from AA and JH are supported by research grants from the Natural Sciences and Engineering Research Council of Canada.

CONFLICT OF INTEREST

Authors have no conflict of interest to declare.

ORCID

David Fernández-Blanco  <https://orcid.org/0000-0002-5326-9164>

REFERENCES

- Abgarmi, B., Delph, J., Ozacar, A., Beck, S., Zandt, G., Sandvol, E., ... Biryol, C. (2017). Structure of the crust and African slab beneath the central Anatolian plateau from receiver functions: New insights on isostatic compensation and slab dynamics. *Geosphere*, *13*, 1774–1787. <https://doi.org/10.1130/GES01509.1>
- Aksu, A., Calon, T., Hall, J., Mansfield, S., & Yaşar, D. (2005). The Cilicia-Adana basin complex, Eastern Mediterranean: Neogene evolution of an active fore-arc basin in an obliquely convergent margin. *Marine Geology*, *221*, 121–159.
- Aksu, A., Calon, T., Hall, J., & Yaşar, D. (2005). Origin and evolution of the Neogene Iskenderun Basin, northeastern Mediterranean Sea. *Marine Geology*, *221*, 161–187.
- Aksu, A., Walsh-Kennedy, S., Hall, J., Hiscott, R., Yalıtırak, C., Akhun, S., & Çifçi, G. (2014). The Pliocene-Quaternary tectonic evolution of the Cilicia and Adana basins, eastern Mediterranean: Special reference to the development of the Kozan Fault zone. *Tectonophysics*, *622*, 22–43. <https://doi.org/10.1016/j.tecto.2014.03.025>
- Allmendinger, R., Jordan, T., Kay, S., & Isacks, B. (1997). The evolution of the Altiplano-Puna plateau of the Central Andes. *Annual Review of Earth and Planetary Sciences*, *25*, 139–174. <https://doi.org/10.1146/annurev.earth.25.1.139>
- Andrew, T., & Robertson, A. (2002). The Beyşehir–Hoyran–Hadım Nappes: Genesis and emplacement of Mesozoic marginal and oceanic units of the northern Neotethys in southern Turkey. *Journal of the Geological Society*, *159*, 529–543. <https://doi.org/10.1144/0016-764901-157>
- Aydar, E. (1998). Early Miocene to Quaternary evolution of volcanism and the basin formation in western Anatolia: A review. *Journal of Volcanology and Geothermal Research*, *85*, 69–82. [https://doi.org/10.1016/S0377-0273\(98\)00050-X](https://doi.org/10.1016/S0377-0273(98)00050-X)
- Bakırcı, T., Yoshizawa, K., & Özer, M. (2012). Three-dimensional S-wave structure of the upper mantle beneath Turkey from surface wave tomography. *Geophysical Journal International*, *190*, 1058–1076. <https://doi.org/10.1111/j.1365-246X.2012.05526.x>
- Ballato, P., Mulch, A., Landgraf, A., Strecker, M., Dalconi, M., Friedrich, A., & Tabatabaei, S. (2010). Middle to late Miocene Middle Eastern climate from stable oxygen and carbon isotope data, southern Alborz mountains, N Iran. *Earth and Planetary Science Letters*, *300*, 125–138. <https://doi.org/10.1016/j.epsl.2010.09.043>
- Bartol, J., & Govers, R. (2014). A single cause for uplift of the Central and Eastern Anatolian plateau? *Tectonophysics*, *637*, 116–136.
- Bassant, P., Van Buchem, F., Strasser, A., & Görür, N. (2005). The stratigraphic architecture and evolution of the Burdigalian carbonate–siliciclastic sedimentary systems of the Mut Basin, Turkey. *Sedimentary Geology*, *173*, 187–232. <https://doi.org/10.1016/j.sedgeo.2004.01.017>
- Bird, P. (1979). Continental delamination and the Colorado Plateau. *Journal of Geophysical Research: Solid Earth*, *84*, 7561–7571. <https://doi.org/10.1029/JB084iB13p07561>
- Biryol, C., Beck, S., Zandt, G., & Özacar, A. (2011). Segmented African lithosphere beneath the Anatolian region inferred from teleseismic P-wave tomography. *Geophysical Journal*, *184*, 1037–1057. <https://doi.org/10.1111/j.1365-246X.2010.04910.x>
- Bridge, C., Calon, T., Hall, J., & Aksu, A. (2005). Salt tectonics in two convergent-margin basins of the Cyprus arc, Northeastern Mediterranean. *Marine Geology*, *221*, 223–259. <https://doi.org/10.1016/j.margeo.2005.03.008>
- Burton-Ferguson, R., Aksu, A., Calon, T., & Hall, J. (2005). Seismic stratigraphy and structural evolution of the Adana Basin, eastern Mediterranean. *Marine Geology*, *221*, 189–222. <https://doi.org/10.1016/j.margeo.2005.03.009>
- Calon, T., Aksu, A., & Hall, J. (2005a). The Neogene evolution of the Outer Latakia Basin and its extension into the Eastern Mesaoria Basin (Cyprus), Eastern Mediterranean. *Marine Geology*, *221*, 61–94.
- Calon, T., Aksu, A., & Hall, J. (2005b). The Oligocene-Recent evolution of the Mesaoria Basin (Cyprus) and its western marine extension, Eastern Mediterranean. *Marine Geology*, *221*, 95–120.
- Çiner, A., Karabiyikoğlu, M., Monod, O., Deynoux, M., & Tuzcu, S. (2008). Late cenozoic sedimentary evolution of the Antalya Basin, Southern Turkey. *Turkish Journal of Earth Sciences*, *17*, 1–41.
- Cipollari, P., Halássová, E., Gürbüz, K., & Cosentino, D. (2013). Middle–Upper Miocene paleogeography of southern Turkey: Insights from stratigraphy and calcareous nannofossil biochronology of the Olukpınar and Başyayla sections (Mut-Ermenek Basin). *Turkish Journal of Earth Sciences*, *22*, 820–838. <https://doi.org/10.3906/yer-1208-2>
- Clark, M. (2012). Continental collision slowing due to viscous mantle lithosphere rather than topography. *Nature*, *483*, 74–77. <https://doi.org/10.1038/nature10848>
- Clark, M., & Robertson, A. (2002). The role of the Early Tertiary Ulukisla Basin, southern Turkey, in suturing of the Mesozoic Tethys Ocean. *Journal of the Geological Society*, *159*, 673–690. <https://doi.org/10.1144/0016-764902-015>
- Clark, M., & Robertson, A. (2005). Uppermost Cretaceous–Lower Tertiary Ulukışla Basin, south-central Turkey: Sedimentary evolution of part of a unified basin complex within an evolving Neotethyan suture zone. *Sedimentary Geology*, *173*, 15–51. <https://doi.org/10.1016/j.sedgeo.2003.12.010>
- Cosentino, D., Buchwaldt, R., Sampalmieri, G., Iadanza, A., Cipollari, P., Schildgen, T., ... Bowring, S. (2013). Refining the Mediterranean “Messinian gap” with high-precision U–Pb zircon geochronology, central and northern Italy. *Geology*, *41*, 323–326. <https://doi.org/10.1130/G33820.1>
- Cosentino, D., Schildgen, T., Cipollari, P., Faranda, C., Gliozzi, E., Hudáčeková, N., ... Strecker, M. (2012). Late Miocene surface uplift of the southern margin of the Central Anatolian Plateau,

- Central Taurides, Turkey. *GSA Bulletin*, 124, 133–145. <https://doi.org/10.1130/B30466.1>
- Delph, J., Abgarmi, B., Ward, K., Beck, S., Özacar, A., Zandt, G., ... Kalafat, D. (2017). The effects of subduction termination on the continental lithosphere: Linking volcanism, deformation, surface uplift, and slab tearing in central Anatolia. *Geosphere*, 13, 1788–1805. <https://doi.org/10.1130/GES01478.1>
- Deniel, C., Aydar, E., & Gourgau, A. (1998). The Hasan Dagı stratovolcano (Central Anatolia, Turkey): Evolution from calc-alkaline to alkaline magmatism in a collision zone. *Journal of Volcanology and Geothermal Research*, 87, 275–302. [https://doi.org/10.1016/S0377-0273\(98\)00097-3](https://doi.org/10.1016/S0377-0273(98)00097-3)
- Dogan-Kulahci, G., Temel, A., Gourgau, A., Varol, E., Guillou, H., & Deniel, C. (2018). Contemporaneous alkaline and calc-alkaline series in Central Anatolia (Turkey): Spatio-temporal evolution of a post-collisional Quaternary basaltic volcanism. *Journal of Volcanology and Geothermal Research*, 356, 56–74. <https://doi.org/10.1016/j.jvolgeores.2018.02.012>
- Eriş, K., Bassant, P., & Ülgen, U. (2005). Tectono-stratigraphic evolution of an Early Miocene incised valley-fill (Derinçay Formation) in the Mut Basin, Southern Turkey. *Sedimentary Geology*, 173, 151–185. <https://doi.org/10.1016/j.sedgeo.2003.12.011>
- Evans, G., Morgan, P., Evans, W., Evans, T., & Woodside, J. (1978). Faulting and halokinetics in the northeastern Mediterranean between Cyprus and Turkey. *Geology*, 6, 392–396. [https://doi.org/10.1130/0091-7613\(1978\)6<392:FAHITN>2.0.CO;2](https://doi.org/10.1130/0091-7613(1978)6<392:FAHITN>2.0.CO;2)
- Faranda, C., Gliozzi, E., Cipollari, P., Grossi, F., Darbaş, G., Gürbüz, K., ... Cosentino, D. (2013). Messinian paleoenvironmental changes in the easternmost Mediterranean Basin: Adana Basin, southern Turkey. *Turkish Journal of Earth Sciences*, 22, 839–863.
- Fernández-Blanco, D. (2014). *Evolution of orogenic plateaus at subduction zones: Sinking and raising the southern margin of the Central Anatolian Plateau*. Ph.D. Thesis Amsterdam: Vrije Universiteit.
- Fernández-Blanco, D., Bertotti, G., Cassola, T., & Willett, S. (2012). *Neogene vertical tectonics of the south margin of the Central Anatolia plateau in relation to Cyprus Arc subduction*. AGU Fall Meeting, San Francisco, CA.
- Fernández-Blanco, D., Bertotti, G., & Çiner, A. (2013). Cenozoic tectonics of the Tuz Gölü Basin (Central Anatolia Plateau, Turkey). *Turkish Journal of Earth Sciences*, 22, 715–738. <https://doi.org/10.3906/yer-1206-7>
- Freund, R. (1979). Progressive strain in beds of monoclinial flexures. *Geology*, 7, 269–271. [https://doi.org/10.1130/0091-7613\(1979\)7<269:PSIBOM>2.0.CO;2](https://doi.org/10.1130/0091-7613(1979)7<269:PSIBOM>2.0.CO;2)
- Fuller, C., Willett, S., & Brandon, M. (2006). Formation of forearc basins and their influence on subduction zone earthquakes. *Geology*, 34, 65–68. <https://doi.org/10.1130/G21828.1>
- Garcia-Castellanos, D. (2007). The role of climate during high plateau formation. Insights from numerical experiments. *Earth and Planetary Science Letters*, 257, 372–390. <https://doi.org/10.1016/j.epsl.2007.02.039>
- Göğüş, O., & Pysklywec, R. (2008). Mantle lithosphere delamination driving plateau uplift and synconvergent extension in eastern Anatolia. *Geology*, 36, 723–726. <https://doi.org/10.1130/G24982A.1>
- Göğüş, O., Pysklywec, R., Şengör, A., & Gün, E. (2017). Drip tectonics and the enigmatic uplift of the Central Anatolian Plateau. *Nature Communications*, 8, 1538. <https://doi.org/10.1038/s41467-017-01611-3>
- Görür, N., Oktay, F., Seymen, I., & Şengör, A. (1984). Palaeotectonic evolution of the Tuzgolu basin complex, Central Turkey: Sedimentary record of a Neo-Tethyan closure. *Geological Society of London Special Publications*, 17, 467–482.
- Gürer, M. (2017). Subduction evolution in the Anatolian region: The rise, demise, and fate of the Anadolu Plate. University Utrecht.
- Hall, J., Aksu, A., Calon, T., & Yaşar, D. (2005). Varying tectonic control on basin development at an active microplate margin: Latakia Basin, Eastern Mediterranean. *Marine Geology*, 221, 15–60.
- Hall, J., Calon, T., Aksu, A., & Meade, S. (2005). Structural evolution of the Latakia Ridge and Cyprus Basin at the front of the Cyprus Arc, Eastern Mediterranean Sea. *Marine Geology*, 221, 261–297.
- Huvaz, O. (2009). Comparative petroleum systems analysis of the interior basins of Turkey: Implications for petroleum potential. *Marine and Petroleum Geology*, 26, 1656–1676. <https://doi.org/10.1016/j.marpetgeo.2009.05.002>
- Ilgar, A., & Nemeč, W. (2005). Early Miocene lacustrine deposits and sequence stratigraphy of the Ermenek Basin, Central Taurides, Turkey. *Sedimentary Geology*, 173, 233–275. <https://doi.org/10.1016/j.sedgeo.2003.07.007>
- Imprescia, P., Pondrelli, S., Vannucci, G., & Gresta, S. (2012). Regional centroid moment tensor solutions in Cyprus from 1977 to the present and seismotectonic implications. *Journal of Seismology*, 16, 147–167. <https://doi.org/10.1007/s10950-011-9254-7>
- Işler, F., Aksu, A., Hall, J., Calon, T., & Yaşar, D. (2005). Neogene development of the Antalya Basin, Eastern Mediterranean: An active forearc basin adjacent to an arc junction. *Marine Geology*, 221, 299–330. <https://doi.org/10.1016/j.margeo.2005.03.006>
- Janson, X., Van Buchem, F., Dromart, G., Eichenseer, H., Dellamonica, X., Boichard, R., ... Eberli, G. (2010). Architecture and facies differentiation within a Middle Miocene carbonate platform, Ermenek, Mut Basin, southern Turkey. *Geological Society, London, Special Publications*, 329, 265–290. <https://doi.org/10.1144/SP329.11>
- Karabıyıköğlü, M., Çiner, A., Monod, O., Deynoux, M., Tuzcu, S., & Örçen, S. (2000). Tectonosedimentary evolution of the Miocene Manavgat Basin, western Taurides, Turkey. *Geological Society, London, Special Publications*, 137, 271–294. <https://doi.org/10.1144/GSL.SP.2000.173.01.14>
- McCay, G. (2010). Tectonic-sedimentary evolution of the Girne (Kyrenia) Range and the Mesarya (Mesaoria) Basin, North Cyprus. PhD Thesis. University of Edinburgh.
- McCay, G., & Robertson, A. (2012). Late Eocene-Neogene sedimentary geology of the Girne (Kyrenia) Range, northern Cyprus: A case history of sedimentation related to progressive and diachronous continental collision. *Sedimentary Geology*, 265, 30–55. <https://doi.org/10.1016/j.sedgeo.2012.03.001>
- McCay, G., Robertson, A., Kroon, D., Raffi, I., Ellam, R., & Necdet, M. (2012). Stratigraphy of Cretaceous to Lower Pliocene sediments in the northern part of Cyprus based on comparative ⁸⁷Sr/⁸⁶Sr isotopic, nannofossil and planktonic foraminiferal dating. *Geological Magazine*, 150, 333–359. <https://doi.org/10.1017/S0016756812000465>
- Meijers, M., Brocard, G., Cosca, M., Lüdecke, T., Teyssier, C., Whitney, D., & Mulch, A. (2018). Rapid late Miocene surface uplift of the Central Anatolian Plateau margin. *Earth and Planetary Science Letters*, 497, 29–41. <https://doi.org/10.1016/j.epsl.2018.05.040>
- Monod, O. (1977). Recherches géologiques dans le Taurus occidental au Sud de Beysehir (Turquie). PhD. Université de Paris-Sud Centre d'Orsay.
- Monod, O., Kuzucuoğulu, C., & Okay, A. (2006). A Miocene palaeovalley network in the Western Taurus (Turkey). *Turkish Journal of Earth Sciences*, 15, 1–23.

- Mulch, A., Graham, S., & Chamberlain, C. (2006). Hydrogen isotopes in Eocene river gravels and paleoelevation of the Sierra Nevada. *Science*, *313*, 87–89. <https://doi.org/10.1126/science.1125986>
- Nelson, K., Zhao, W., Brown, L., Kuo, J., Che, J., Liu, X., ... Edwards, M. (1996). Partially molten middle crust beneath Southern Tibet: Synthesis of project INDEPTH results. *Science*, *274*, 1684–1688. <https://doi.org/10.1126/science.274.5293.1684>
- Öğretmen, N., Cipollari, P., Frezza, V., Faranda, C., Karanika, K., Gliozzi, E., ... Cosentino, D. (2018). Evidence for 1.5 km of uplift of the Central Anatolian Plateau's Southern Margin in the Last 450 kyr and Implications for Its Multiphased Uplift History. *Tectonics*, *2017TC004805*.
- Özsayin, E., Ciner, A., Rojay, B., Dirik, K., Melnick, D., Fernández-Blanco, D., ... Sudo, (2013). Plio-Quaternary extensional tectonics of the Central Anatolian Plateau: A case study from the Tuz Gölü Basin, Turkey. *Turkish Journal of Earth Sciences*, *22*, 691–714.
- Patton, T. (2004). Numerical models of growth-sediment development above an active monocline. *Basin Research*, *16*, 25–39. <https://doi.org/10.1111/j.1365-2117.2003.00220.x>
- Pavlis, T., & Bruhn, R. (1983). Deep-seated flow as a mechanism for the uplift of broad forearc ridges and its role in the exposure of high P/T metamorphic terranes. *Tectonics*, *2*, 473–497. <https://doi.org/10.1029/TC002i005p00473>
- Pope, D., & Willett, S. (1998). Thermal-mechanical model for crustal thickening in the central Andes driven by ablative subduction. *Geology*, *26*, 511–514. [https://doi.org/10.1130/0091-7613\(1998\)026<0511:TMMFCT>2.3.CO;2](https://doi.org/10.1130/0091-7613(1998)026<0511:TMMFCT>2.3.CO;2)
- Portner, D., Delph, J., Biryol, C., Beck, S., Zandt, G., Özacar, A., ... Türkelli, N. (2018). Subduction termination through progressive slab deformation across Eastern Mediterranean subduction zones from updated P-wave tomography beneath Anatolia. *Geosphere*, *14*, 907–925. <https://doi.org/10.1130/GES01617.1>
- Powell, C. (1986). Continental underplating model for the rise of the Tibetan Plateau. *Earth and Planetary Science Letters*, *81*, 79–94. [https://doi.org/10.1016/0012-821X\(86\)90102-0](https://doi.org/10.1016/0012-821X(86)90102-0)
- Reches, Z., Hoexter, D., & Hirsch, F. (1981). The structure of a monocline in the Syrian Arc system, Middle East-Surface and subsurface analysis. *Journal of Petroleum Geology*, *3*, 413–426. <https://doi.org/10.1111/j.1747-5457.1981.tb00939.x>
- Riba, O. (1976). Syntectonic unconformities of the Alto Cardener, Spanish Pyrenees: A genetic interpretation. *Sedimentary Geology*, *15*, 213–233. [https://doi.org/10.1016/0037-0738\(76\)90017-8](https://doi.org/10.1016/0037-0738(76)90017-8)
- Robertson, A. (1998). Mesozoic-Tertiary tectonic evolution of the easternmost Mediterranean area: integration of marine and land evidence. Proceedings of the Ocean Drilling Program, Scientific Results, Vol. 160; Chapter 54.
- Rowley, D., & Currie, B. (2006). Palaeo-altimetry of the late Eocene to Miocene Lunpola basin, central Tibet. *Nature*, *439*, 677–681. <https://doi.org/10.1038/nature04506>
- Şafak, Ü., Kelling, G., Gökçen, N., & Gürbüz, K. (2005). The mid-Cenozoic succession and evolution of the Mut basin, southern Turkey, and its regional significance. *Sedimentary Geology*, *173*, 121–150. <https://doi.org/10.1016/j.sedgeo.2004.03.012>
- Schildgen, T., Yıldırım, C., Cosentino, D., & Strecker, M. (2014). Linking slab break-off, Hellenic trench retreat, and uplift of the Central and Eastern Anatolian plateaus. *Earth-Science Reviews*, *128*, 147–168. <https://doi.org/10.1016/j.earscirev.2013.11.006>
- Schildgen, T., Cosentino, D., Bookhagen, B., Niedermann, S., Yıldırım, C., Echtler, H., ... Strecker, M. (2012). Multi-phased uplift of the southern margin of the Central Anatolian plateau, Turkey: A record of tectonic and upper mantle processes. *Earth and Planetary Science Letters*, *317–318*, 85–95. <https://doi.org/10.1016/j.epsl.2011.12.003>
- Şengör, A., Özeren, S., Genç, T., & Zor, E. (2003). East Anatolian high plateau as a mantle-supported, north-south shortened domal structure. *Geophysical Research Letters*, *30*, 1–12. <https://doi.org/10.1029/2003GL017858>
- Sobel, E., Hillel, G., & Strecker, M. (2003). Formation of internally drained contractional basins by aridity-limited bedrock incision. *Journal of Geophysical Research: Solid Earth*, *108*(B7). <https://doi.org/10.1029/2002JB001883>
- Strecker, M., Alonso, R., Bookhagen, B., Carrapa, B., Coutand, I., Hain, M., ... Sobel, E. (2009). Does the topographic distribution of the central Andean Puna Plateau result from climatic or geodynamic processes? *Geology*, *37*, 643–646.
- Tapponnier, P., Zhiqin, X., Roger, F., Meyer, B., Arnaud, N., Wittlinger, G., & Jingsui, Y. (2001). Oblique stepwise rise and growth of the Tibet plateau. *Science*, *294*, 1671–1677. <https://doi.org/10.1126/science.105978>
- Tindall, S., & Davis, G. (1999). Monocline development by oblique-slip fault-propagation folding: The East Kaibab monocline, Colorado Plateau, Utah. *Journal of Structural Geology*, *21*, 1303–1320. [https://doi.org/10.1016/S0191-8141\(99\)00089-9](https://doi.org/10.1016/S0191-8141(99)00089-9)
- Ulü, Ü. (2002). Geological map of Turkey, Adana (No. 15): Maden Tetkik ve Arama Genel Müdürlüğü (MTA), M. Şenel (Ed.), scale 1:500,000, 1 sheet.
- Walsh-Kennedy, S., Aksu, A., Hall, J., Hiscott, R., Yaltrak, C., & Çifçi, G. (2014). Source to sink: The development of the latest Messinian to Pliocene-Quaternary Cilicia and Adana Basins and their linkages with the onland Mut Basin, eastern Mediterranean. *Tectonophysics*, *622*, 1–21. <https://doi.org/10.1016/j.tecto.2014.01.019>
- Willett, S., & Schlunegger, F. (2010). The last phase of deposition in the Swiss Molasse Basin: From foredeep to negative-alpha basin. *Basin Research*, *22*, 623–639. <https://doi.org/10.1111/j.1365-2117.2009.00435.x>
- Willsey, S. P., Umhoefer, P. J., & Hillel, G. E. (2002). Early evolution of an extensional monocline by a propagating normal fault: 3D analysis from combined field study and numerical modeling. *Journal of Structural Geology*, *24*, 651–669. [https://doi.org/10.1016/S0191-8141\(01\)00120-1](https://doi.org/10.1016/S0191-8141(01)00120-1)
- Yetiş, C., Kelling, G., Gökçen, S. L., & Baroz, F. (1995). A revised stratigraphic framework for Later Cenozoic sequences in the northeastern Mediterranean region. *Geologische Rundschau: Zeitschrift Fur Allgemeine Geologie*, *84*, 794. <https://doi.org/10.1007/BF00240569>
- Yin, A., & Harrison, T. M. (2000). Geologic Evolution of the Himalayan-Tibetan Orogen. *Annual Review of Earth and Planetary Sciences*, *28*, 211–280. <https://doi.org/10.1146/annurev.earth.28.1.211>

SUPPORTING INFORMATION

Additional supporting information may be found online in the Supporting Information section at the end of the article.

How to cite this article: Fernández-Blanco D, Bertotti G, Aksu A, Hall J. Monoclinial flexure of an orogenic plateau margin during subduction, south Turkey. *Basin Res.* 2019;31:709–727. <https://doi.org/10.1111/bre.12341>